Consistent microscopic analysis of spin pumping effects

Gen Tatara
RIKEN Center for Emergent Matter Science (CEMS), 2-1 Hirosawa, Wako, Saitama 351-0198, Japan

Shigemi Mizukami
WPI - Advanced Insitute for Materials Research, Tohoku University Katahira 2-1-1, Sendai, Japan

(Received 2 June 2017; revised manuscript received 28 July 2017; published 18 August 2017)

We present a consistent microscopic study of spin pumping effects for both metallic and insulating ferromagnets. As for the metallic case, we present a simple quantum mechanical picture of the effect as due to the electron spin flip as a result of a nonadiabatic (off-diagonal) spin gauge field. The effect of interface spin-orbit interaction is briefly discussed. We also carry out a field-theoretic calculation to discuss on equal footing the spin current generation and torque effects such as an enhanced Gilbert damping constant and a shift of precession frequency both in metallic and insulating cases. For thick ferromagnetic metals, our study reproduces the results of previous theories such as the correspondence between the dc component of the spin current and the enhancement of the damping. For thin metals and insulators, the relation turns out to be modified. For the insulating case, driven locally by interface *sd* exchange interaction due to magnetic proximity effect, the physical mechanism is distinct from the metallic case. Further study of the proximity effect and interface spin-orbit interaction would be crucial to interpret experimental results in particular for insulators.

DOI: 10.1103/PhysRevB.96.064423

I. INTRODUCTION

Spin current generation is of a fundamental importance in spintronics. A dynamic method using magnetization precession induced by an applied magnetic field, called the spin pumping effect, turns out to be particularly useful [1] and is widely used in a junction of a ferromagnet (F) and a normal metal (N) (Fig. 1). The generated spin current density (in unit of A/m^2) has two independent components, proportional to $\dot{\boldsymbol{n}}$ and $\boldsymbol{n}\times\dot{\boldsymbol{n}}$, where $\boldsymbol{n}$ is a unit vector describing the direction of localized spin, and thus is represented phenomenologically as

$$\boldsymbol{j}_s = \frac{e}{4\pi}(A_{\rm r}\boldsymbol{n}\times\dot{\boldsymbol{n}} + A_{\rm i}\dot{\boldsymbol{n}}), \tag{1}$$

where e is the elementally electric charge and $A_{\rm r}$ and $A_{\rm i}$ are phenomenological constants having unit of $1/{\rm m}^2$. The spin pumping effect was theoretically formulated by Tserkovnyak *et al.* [2] by use of the scattering matrix approach [3]. This approach, widely applied in mesoscopic physics, describes transport phenomena in terms of transmission and reflection amplitudes (scattering matrix), and provides a quantum mechanical picture of the phenomena without calculating explicitly the amplitudes. Tserkovnyak *et al.* applied the scattering matrix formulation of general adiabatic pumping [4,5] to the spin-polarized case. The spin pumping effect was described in Ref. [2] in terms of spin-dependent transmission and reflection coefficients at the FN interface, and it was demonstrated that the two parameters, $A_{\rm r}$ and $A_{\rm i}$, are the real and the imaginary parts of a complex parameter called the spin mixing conductance. The spin mixing conductance, which is represented by transmission and reflection coefficients, turned out to be a convenient parameter for discussing spin current generation and other effects like the inverse spin-Hall effect. Nevertheless, the scattering approach hides the microscopic physical picture of what is going on, as the scattering coefficients are not fundamental material parameters but are composite quantities of the Fermi wave vector, the electron effective mass, and the interface properties.

The effects of a slowly varying potential are described in a physically straightforward and clear manner by the use of a unitary transformation that represents the time dependence (see Sec. II A for details). The laboratory frame wave function under a time-dependent potential $|\psi(t)\rangle$ is written in terms of a static ground state ("rotated-frame" wave function) $|\phi\rangle$ and a unitary matrix $U(t)$ as $|\psi(t)\rangle = U(t)|\phi\rangle$. The time derivative ∂_t is then replaced by a covariant derivative $\partial_t + (U^{-1}\partial_t U)$, and the effects of time dependence are represented by (the time component of) an effective gauge field, $\mathcal{A} \equiv -i(U^{-1}\partial_t U)$ [see Eq. (12)]. In the same manner as the electromagnetic gauge field, the effective gauge field generates a current if spatial inhomogeneity is present (like in junctions), and this is the physical origin of the pumping effect in metals.

It should be noted that the effective gauge field that drives spin current is a nonadiabatic one, off-diagonal in spin, and not the adiabatic gauge field that induces spin Berry's phase, the spin motive force, and spin transfer effects. Nevertheless, the pumping efficiency can be calculated within an adiabatic pumping scheme, as shall be discussed in Sec. II C.

In the perturbative regime or in insulators, a simple picture instead of an effective gauge field can be presented. Let us focus on the case driven by an *sd* exchange interaction, $J_{sd}\boldsymbol{n}(t)\cdot\boldsymbol{\sigma}$, where J_{sd} is a coupling constant and $\boldsymbol{\sigma}$ is the electron spin. Considering the second-order effect of the *sd* exchange interaction, the electron wave function has a contribution of a time-dependent amplitude

$$\begin{aligned}\mathcal{U}(t_1,t_2) &= (J_{sd})^2(\boldsymbol{n}(t_1)\cdot\boldsymbol{\sigma})(\boldsymbol{n}(t_2)\cdot\boldsymbol{\sigma}) \\ &= (J_{sd})^2\{(\boldsymbol{n}(t_1)\cdot\boldsymbol{n}(t_2)) + i[\boldsymbol{n}(t_1)\times\boldsymbol{n}(t_2)]\cdot\boldsymbol{\sigma}\},\end{aligned} \tag{2}$$

where t_1 and t_2 are the times of the interactions. The first term on the right-hand side, representing the amplitude for charge degrees of freedom, is neglected. The spin contribution vanishes for a static spin configuration, as is natural, while for

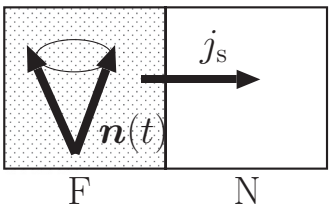

FIG. 1. Spin pumping effect in a junction of ferromagnet (F) and normal metal (N). Dynamic magnetization $\boldsymbol{n}(t)$ generates a spin current j_s through the interface.

the slowly varying case, it reads

$$\mathcal{U}(t_1,t_2) \simeq -i(t_1-t_2)(J_{sd})^2(\boldsymbol{n}\times\dot{\boldsymbol{n}})(t_1)\cdot\boldsymbol{\sigma}. \tag{3}$$

As a result of this amplitude, spin accumulation and spin current is induced proportional to $\boldsymbol{n}\times\dot{\boldsymbol{n}}$. This fact indicates that $\boldsymbol{n}\times\dot{\boldsymbol{n}}$ plays a role of an effective scalar potential or voltage in electromagnetism, as we shall demonstrate in Sec. VII B for insulators. [The factor of time difference is written in terms of a derivative with respect to energy or angular frequency in a rigorous derivation. See, for example, Eqs. (E6) and (E9).] The essence of the spin pumping effect is therefore the noncommutativity of spin operators. The above picture in the perturbative regime naturally leads to the effective gauge field picture in the strong-coupling limit [6].

The same scenario applies for cases of spatial variation of spin, and an equilibrium spin current proportional to $\boldsymbol{n}\times\nabla_i\boldsymbol{n}$ emerges, where i denotes the direction of spatial variation [7]. The spin pumping effect is therefore the time analog of the equilibrium spin current induced by vector spin chirality. Moreover, a charge current emerges from the third-order process from the identity [6]

$$\mathrm{tr}[(\boldsymbol{n}_1\cdot\boldsymbol{\sigma})(\boldsymbol{n}_2\cdot\boldsymbol{\sigma})(\boldsymbol{n}_3\cdot\boldsymbol{\sigma})] = 2i\boldsymbol{n}_1\cdot(\boldsymbol{n}_2\times\boldsymbol{n}_3), \tag{4}$$

and this factor, a scalar spin chirality, is the analog of the spin Berry phase in the perturbative regime. The spin pumping effect, spin Berry's phase, and the spin motive force have the same physical root, namely, the noncommutative spin algebra.

From the scattering matrix theory view point, the cases of metallic and insulating ferromagnet make no difference since what the conduction electrons in the normal metal see is the interface. From the physical viewpoint, such treatment appears too crude. Unlike the metallic case discussed above, in the case of an insulator ferromagnet, the coupling between the magnetization and the conduction electron in a normal metal occurs due to a magnetic proximity effect at the interface, as is experimentally indicated [8]. Thus the spin pumping by an insulator ferromagnet is a locally induced perturbative effect rather than a transport induced by a driving force due to a generalized gauge field. We therefore need to apply different approaches for the two cases. In the insulating case, one may think that a magnon spin current is generated inside the ferromagnet because the magnons couple to an effective gauge field [9] similarly to the electrons in metallic case. This is not, however, true, because the gauge field for magnons is Abelian [U(1)], and has no off-diagonal "spin-flip" component. Although the scattering matrix approach apparently seems to apply to both metallic and insulating cases, it would be instructive to present in this paper a consistent microscopic description of the effects to see the different physics governing the two cases.

A. Brief overview of theories and scope of the paper

Before carrying out calculations, let us overview the history of theoretical studies of the spin pumping effect. Spin current generation in a metallic junction was originally discussed by Silsbee *et al.* [10] before Tserkovnyak *et al.* It was shown there that dynamic magnetization induces spin accumulation at the interface, resulting in a diffusive flow of spins in the normal metal. Although at that time the experimental interest was focused on the interface spin accumulation, which enhances the signal of conduction electron spin resonance, it would be fair to say that Silsbee *et al.* pointed out the "spin pumping effect".

In Ref. [2], the spin pumping effect was originally argued in the context of enhancement of Gilbert damping in an FN junction, which had been a hot issue after the study by Berger [11], who studied the case of FNF junctions based on a quantum mechanical argument. Berger discussed that when a normal metal is attached to a ferromagnet, the damping of the ferromagnet is enhanced as a result of spin polarization formed in the normal metal, and the effect was experimentally confirmed by Mizukami *et al.* [12]. Tserkovnyak *et al.* pointed out that the effect can be interpreted as the counteraction of spin current generation, because the spin current injected into the normal metal indicates emergence of a torque for the ferromagnet. In fact, the equation of motion for the magnetization of ferromagnet reads

$$\dot{\boldsymbol{n}} = -\gamma\boldsymbol{B}\times\boldsymbol{n} - \alpha\boldsymbol{n}\times\dot{\boldsymbol{n}} - \frac{a^3}{eSd}\boldsymbol{j}_s, \tag{5}$$

where γ is the gyromagnetic ratio, α is the Gilbert damping coefficient, d is the thickness of the ferromagnet, S is the magnitude of localized spin, and a is the lattice constant. The spin current of Eq. (1) thus indicates that the gyromagnetic ratio and the Gilbert damping coefficient are modified by the spin pumping effect to be [2]

$$\tilde{\alpha} = \alpha + \frac{a^3}{4\pi Sd}A_r,$$
$$\tilde{\gamma} = \gamma\left(1+\frac{a^3}{4\pi Sd}A_i\right)^{-1}. \tag{6}$$

The spin pumping effect is therefore detected by measuring the effective damping constant and gyromagnetic ratio. Formula (6) is, however, based on a naive picture neglecting the position dependence of the damping torque and the relation between the pumped spin current amplitude and damping, or γ would not be so simple in reality (see Sec. V).

The issue of damping in an FN junction was formulated based on linear-response theory by Simanek and Heinirch [13,14]. They showed that the damping coefficient is given by the first-order derivative with respect to the angular frequency ω of the imaginary part of the spin correlation function and argued that the damping effect is consistent with Tserkovnyak's spin pumping effect. Recently, a microscopic formulation of spin pumping effect in metallic junctions was

provided by Chen and Zhang [15] and one of the authors of Ref. [16] by use of the Green's functions, and a transparent microscopic picture of pumping effect was provided. The scattering representation and the Green's function one are related [15] because the asymptotic behaviors of the Green's functions at long distance are governed by the transmission coefficient [17]. In the study of Ref. [16], the uniform ferromagnet was treated as a dot having only two degrees of freedom of spin. Such simplification neglects the dependence on electron wave vectors in ferromagnets and thus cannot discuss the case of inhomogeneous magnetization or position dependence of spin damping.

The aim of this paper is to provide a microscopic and consistent theoretical formulation of spin pumping effect for metallic and insulating ferromagnets. We do not rely on the scattering approach. Instead, we provide an elementary quantum mechanical argument to demonstrate that spin current generation is a natural consequence of magnetization dynamics (Sec. II). Based on the formulation, the effect of interface spin-orbit interaction is discussed in Sec. III. We also provide a rigorous formulation based on the field-theoretic approach employed in Ref. [16] in Sec. IV. We also reproduce within the same framework Berger's result [11] that the spin pumping effect is equivalent to the enhancement of the spin damping (Sec. V). The effect of inhomogeneous magnetization is briefly discussed in Sec. VI.

The case of insulating ferromagnet is studied in Sec. VII assuming that the pumping is induced by an interface exchange interaction between the magnetization and conduction electrons in a normal metal, namely, by the magnetic proximity effect [8]. The interaction is treated perturbatively similarly to Refs. [18,19]. The dominant contribution to the spin current, the one linear in the interface exchange interaction, turns out to be proportional to $\dot{\boldsymbol{n}}$, while the one proportional to $\boldsymbol{n}\times\dot{\boldsymbol{n}}$ is weaker if the proximity effect is weak.

The contribution from the magnons, magnetization fluctuations, is also studied. As has been argued [9], a gauge field for magnons emerges from magnetization dynamics. It is, however, an adiabatic one, diagonal in spin, which acts as a chemical potential for magnons, giving rise only to adiabatic spin polarization proportional to $\boldsymbol{n}$. This is in sharp contrast to the metallic case, where electrons are directly driven by the spin-flip component of the spin gauge field, resulting in perpendicular spin accumulation, i.e., along $\dot{\boldsymbol{n}}$ and $\boldsymbol{n}\times\dot{\boldsymbol{n}}$. The excitation in a ferromagnet when the magnetization is time-dependent is therefore different for the metallic and the insulating cases. We show that a magnon excitation nevertheless generates perpendicular spin current, $\boldsymbol{n}\times\dot{\boldsymbol{n}}$, in the normal metal as a result of annihilation and creation at the interface, which in turn flips the electron spin. The result of the magnon-driven contribution agrees with the one in the previous study [20] carried out in the context of thermally driven spin pumping ("spin Seebeck" effect). It is demonstrated that the magnon-induced spin current depends linearly on the temperature at high temperature compared to magnon energy. The amplitude of magnon-driven spin current provides the magnitude of the magnetic proximity effect.

In our analysis, we calculate consistently the pumped spin current and change of the Gilbert damping and resonant frequency and obtain the relations among them. It is shown that the spin mixing conductance scenario saying that the magnitude of spin current proportional to $\boldsymbol{n}\times\dot{\boldsymbol{n}}$ is given by the enhancement factor of the Gilbert damping constant [2], applies only in the case of thick ferromagnetic metals. For the thin metallic and insulator cases, different relations hold (see Sec. VIII).

II. QUANTUM MECHANICAL DESCRIPTION OF METALLIC CASE

In this section, we derive the spin current generated by the magnetization dynamics of a metallic ferromagnet by a quantum mechanical argument. It is sometimes useful for intuitive understanding, although the description may lack clearness as it cannot handle many-particle aspects like particle distributions. In Sec. IV, we formulate the problem in the field-theoretic language.

A. Electrons in ferromagnet with dynamic magnetization

The model we consider is a junction of a metallic ferromagnet (F) and a normal metal (N). The magnetization (or localized spins) in the ferromagnet is treated as spatially uniform but changing with time slowly. As a result of strong sd exchange interaction, the conduction electron's spin follows instantaneous directions of localized spins, i.e., the system is in the adiabatic limit. The quantum mechanical Hamiltonian for the ferromagnet is

$$H_{\rm F}=-\frac{\nabla^2}{2m}-\epsilon_F-M\boldsymbol{n}(t)\cdot\boldsymbol{\sigma}, \tag{7}$$

where m is the electron mass, $\boldsymbol{\sigma}$ is a vector of Pauli matrices, M represents the energy splitting due to the sd exchange interaction, and $\boldsymbol{n}(t)$ is a time-dependent unit vector denoting the localized spin direction. The energy is measured from the Fermi energy ϵ_F.

As a result of the sd exchange interaction, the electron's spin wave function is given by [21]

$$|\boldsymbol{n}\rangle\equiv\cos\frac{\theta}{2}|\uparrow\rangle+\sin\frac{\theta}{2}e^{i\phi}|\downarrow\rangle, \tag{8}$$

where $|\uparrow\rangle$ and $|\downarrow\rangle$ represent the spin-up and -down states, respectively, and (θ,ϕ) are polar coordinates for $\boldsymbol{n}$. To treat slowly varying localized spins, we switch to a rotated frame where the spin direction is defined with respect to an instantaneous direction $\boldsymbol{n}$ [7]. This corresponds to diagonalizing the Hamiltonian at each time by introducing a unitary matrix $U(t)$ as

$$|\boldsymbol{n}(t)\rangle\equiv U(t)|\uparrow\rangle, \tag{9}$$

where

$$U(t)=\begin{pmatrix}\cos\frac{\theta}{2} & \sin\frac{\theta}{2}e^{-i\phi}\\ \sin\frac{\theta}{2}e^{i\phi} & -\cos\frac{\theta}{2}\end{pmatrix}, \tag{10}$$

where states are in vector representation, i.e., $|\uparrow\rangle=\binom{1}{0}$ and $|\downarrow\rangle=\binom{0}{1}$. In the rotated frame, the Hamiltonian is diagonalized as (in the momentum representation)

$$\widetilde{H}_{\rm F}\equiv U^{-1}H_{\rm F}U=\epsilon_{\boldsymbol{k}}-M\sigma_z, \tag{11}$$

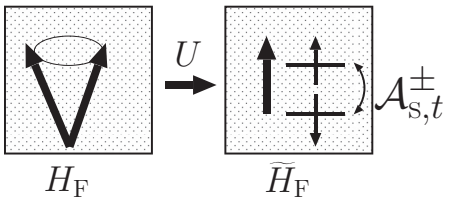

FIG. 2. Unitary transformation U for conduction electrons in a ferromagnet converts the original Hamiltonian H_{F} into a diagonalized uniformly spin-polarized Hamiltonian $\widetilde{H}_{\mathrm{F}}$ and an interaction with a spin gauge field, $\boldsymbol{\mathcal{A}}_{\mathrm{s},t}\cdot\boldsymbol{\sigma}$.

where $\epsilon_{\boldsymbol{k}} \equiv \frac{k^2}{2m} - \epsilon_F$ is the kinetic energy in the momentum representation (Fig. 2). In general, when a state $|\psi\rangle$ for a time-dependent Hamiltonian $H(t)$, satisfying the Schrödinger equation $i\frac{\partial}{\partial t}|\psi\rangle = H(t)|\psi\rangle$, is written in terms of a state $|\psi\rangle$ connected by a unitary transformation $|\phi\rangle \equiv U^{-1}|\psi\rangle$, the new state satisfies a modified Schrödinger equation:

$$\left(i\frac{\partial}{\partial t} + iU^{-1}\frac{\partial}{\partial t}U\right)|\phi\rangle = \tilde{H}|\phi\rangle, \tag{12}$$

where $\tilde{H} \equiv U^{-1}HU$. Namely, there arises a gauge field $-iU^{-1}\frac{\partial}{\partial t}U$ in the new frame $|\phi\rangle$. In the present case of dynamic localized spin, the gauge field has three components (suffix t denotes the time component):

$$\mathcal{A}_{\mathrm{s},t} \equiv -iU^{-1}\frac{\partial}{\partial t}U \equiv \boldsymbol{\mathcal{A}}_{\mathrm{s},t}\cdot\boldsymbol{\sigma}, \tag{13}$$

explicitly given as [7]

$$\boldsymbol{\mathcal{A}}_{\mathrm{s},t} = \frac{1}{2}\begin{pmatrix} -\partial_t\theta\sin\phi - \sin\theta\cos\phi\partial_t\phi \\ \partial_t\theta\cos\phi - \sin\theta\sin\phi\partial_t\phi \\ (1-\cos\theta)\partial_t\phi \end{pmatrix}. \tag{14}$$

Including the gauge field in the Hamiltonian, the effective Hamiltonian in the rotated frame reads

$$\widetilde{H}^{\mathrm{eff}}_{\mathrm{F}} \equiv \widetilde{H}_{\mathrm{F}} + \mathcal{A}_{\mathrm{s},t}\cdot\boldsymbol{\sigma} = \begin{pmatrix} \epsilon_k - M - \mathcal{A}^z_{\mathrm{s},t} & \mathcal{A}^-_{\mathrm{s},t} \\ \mathcal{A}^+_{\mathrm{s},t} & \epsilon_k + M + \mathcal{A}^z_{\mathrm{s},t} \end{pmatrix}, \tag{15}$$

where $\mathcal{A}^{\pm}_{\mathrm{s},t} \equiv \mathcal{A}^x_{\mathrm{s},t} \pm i\mathcal{A}^y_{\mathrm{s},t}$. We see that the adiabatic (z) component of the gauge field, $\mathcal{A}^z_{\mathrm{s},t}$, acts as a spin-dependent chemical potential (spin chemical potential) generated by dynamic magnetization, while the nonadiabatic (x and y) components cause spin mixing. In the case of the uniform magnetization we consider, the mixing is between the electrons with different spin $\uparrow$ and $\downarrow$ but with the same wave vector $\boldsymbol{k}$, because the gauge field $\mathcal{A}^{\pm}_{\mathrm{s},t}$ carries no momentum. This leads to a mixing of states having an excitation energy of M as shown in Fig. 3. In low-energy transport effects, what matters are the electrons at the Fermi energy; the wave vector $\boldsymbol{k}$ should be chosen as k_{F+} and k_{F-}, the Fermi wave vectors for $\uparrow$ and $\downarrow$ electrons, respectively. (Effects of finite momentum transfer are discussed in Sec. VI.)

Hamiltonian (15) is diagonalized to obtain energy eigenvalues of $\tilde{\epsilon}_{k\sigma} = \epsilon_{\boldsymbol{k}} - \sigma\sqrt{(M+\mathcal{A}^z_{\mathrm{s},t})^2 + |\mathcal{A}^{\perp}_{\mathrm{s},t}|^2}$, where $|\mathcal{A}^{\perp}_{\mathrm{s},t}|^2 \equiv \mathcal{A}^+_{\mathrm{s},t}\mathcal{A}^-_{\mathrm{s},t}$ and $\sigma = \pm$ represents spin ($\uparrow$ and $\downarrow$ correspond to $+$ and $-$, respectively). We are interested in the adiabatic limit,

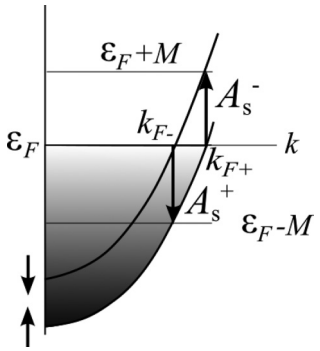

FIG. 3. For uniform magnetization, the nonadiabatic components of the gauge field $\mathcal{A}^{\pm}_{\mathrm{s},t}$ induce a spin flip conserving the momentum.

and so the lowest order contribution, namely, the first order, in the perpendicular component $\mathcal{A}^{\perp}_{\mathrm{s},t}$, is sufficient. In the present rotated-frame approach, the gauge field is treated as a static potential, since it already includes the time derivative to the linear order [see Eq. (14)]. Moreover, the adiabatic component of the gauge field, $\mathcal{A}^z_{\mathrm{s},t}$, is neglected, as it modifies the spin pumping only at the second order of the time derivative. The energy eigenvalues $\epsilon_{\boldsymbol{k}\sigma} \simeq \epsilon_{\boldsymbol{k}} - \sigma M$ are thus unaffected by the gauge field, while the eigenstates to the linear order read

$$\begin{aligned} |k\uparrow\rangle_{\mathrm{F}} &\equiv |k\uparrow\rangle - \frac{\mathcal{A}^+_{\mathrm{s},t}}{M}|k\downarrow\rangle, \\ |k\downarrow\rangle_{\mathrm{F}} &\equiv |k\downarrow\rangle + \frac{\mathcal{A}^-_{\mathrm{s},t}}{M}|k\uparrow\rangle, \end{aligned} \tag{16}$$

corresponding to the energy of $\epsilon_{\boldsymbol{k}+}$ and $\epsilon_{\boldsymbol{k}-}$, respectively. For low-energy transport, the states that we need to consider are the following two, having spin-dependent Fermi wave vectors $k_{F\sigma}$ for $\sigma = \uparrow,\downarrow$, namely,

$$\begin{aligned} \left|k_{\mathrm{F}\uparrow}\uparrow\right\rangle_{\mathrm{F}} &= \left|k_{\mathrm{F}\uparrow}\uparrow\right\rangle - \frac{\mathcal{A}^+_{\mathrm{s},t}}{M}\left|k_{\mathrm{F}\uparrow}\downarrow\right\rangle, \\ \left|k_{\mathrm{F}\downarrow}\downarrow\right\rangle_{\mathrm{F}} &= \left|k_{\mathrm{F}\downarrow}\downarrow\right\rangle + \frac{\mathcal{A}^-_{\mathrm{s},t}}{M}\left|k_{\mathrm{F}\downarrow}\uparrow\right\rangle. \end{aligned} \tag{17}$$

B. Spin current induced in the normal metal

The spin pumping effect is now studied by taking account of the interface hopping effects on the states of Eq. (17) to the linear order. The interface hopping amplitude of electrons in F to N with spin σ is denoted by $\tilde{t}_\sigma$ and the amplitude from N to F is $\tilde{t}^*_\sigma$. We assume that the spin dependence of the electron state in F is governed by the relative angle to the magnetization vector, and hence the spin σ is the one in the rotated frame. Assuming, moreover, that there is no spin-flip scattering at the interface, the amplitude $\tilde{t}_\sigma$ is diagonal in spin. (Interface spin-orbit interaction is considered in Sec. III.) The spin-wave function formed in the N region at the interface as a result of the state in F [Eq. (17)] is then

$$\begin{aligned} |k_F\uparrow\rangle_{\mathrm{N}} &\equiv \tilde{t}|k_F\uparrow\rangle = \tilde{t}_\uparrow|k_F\uparrow\rangle - \tilde{t}_\downarrow\frac{\mathcal{A}^+_{\mathrm{s},t}}{M}|k_F\downarrow\rangle \\ |k_F\downarrow\rangle_{\mathrm{N}} &\equiv \tilde{t}|k_F\downarrow\rangle = \tilde{t}_\downarrow|k_F\downarrow\rangle + \tilde{t}_\uparrow\frac{\mathcal{A}^-_{\mathrm{s},t}}{M}|k_F\uparrow\rangle, \end{aligned} \tag{18}$$

where k_F is the Fermi wave vector of an N electron. The spin density induced in N region at the interface is therefore

$$\tilde{\boldsymbol{s}}^{(\mathrm{N})} = \tfrac{1}{2}({}_{\mathrm{N}}\langle k_F\uparrow|\boldsymbol{\sigma}|k_F\uparrow\rangle_{\mathrm{N}}\nu_\uparrow + {}_{\mathrm{N}}\langle k_F\downarrow|\boldsymbol{\sigma}|k_F\downarrow\rangle_{\mathrm{N}}\nu_\downarrow), \quad (19)$$

where ν_σ is the spin-dependent density of states of F electrons at the Fermi energy. It reads

$$\tilde{\boldsymbol{s}}^{(\mathrm{N})} = \frac{1}{2}\sum_\sigma \nu_\sigma T_{\sigma\sigma}\hat{\boldsymbol{z}} - \frac{\nu_\uparrow - \nu_\downarrow}{M}(\mathrm{Re}[T_{\uparrow\downarrow}]\mathcal{A}^\perp_{\mathrm{s},t} + \mathrm{Im}[T_{\uparrow\downarrow}](\hat{\boldsymbol{z}}\times\mathcal{A}^\perp_{\mathrm{s},t})), \quad (20)$$

where $\boldsymbol{\mathcal{A}}^\perp_{\mathrm{s},t} = (\mathcal{A}^x_{\mathrm{s},t}, \mathcal{A}^y_{\mathrm{s},t}, 0) = \boldsymbol{\mathcal{A}}_{\mathrm{s},t} - \hat{\boldsymbol{z}}\mathcal{A}^z_{\mathrm{s},t}$ is the transverse (nonadiabatic) components of spin gauge field and

$$T_{\sigma\sigma'} \equiv \tilde{t}^*_\sigma \tilde{t}_{\sigma'}. \quad (21)$$

The spin density of Eq. (20) is in the rotated frame. The spin polarization in the laboratory frame is obtained by a rotation matrix $\mathcal{R}_{ij}$, defined by

$$U^{-1}\sigma_i U \equiv \mathcal{R}_{ij}\sigma_j, \quad (22)$$

as

$$s^{(\mathrm{N})}_i = \mathcal{R}_{ij}\tilde{s}^{(\mathrm{N})}_j. \quad (23)$$

Explicitly, $\mathcal{R}_{ij} = 2m_i m_j - \delta_{ij}$, where $\boldsymbol{m} \equiv (\sin\frac{\theta}{2}\cos\phi, \sin\frac{\theta}{2}\sin\phi, \cos\frac{\theta}{2})$ [7]. Using

$$\mathcal{R}_{ij}(\boldsymbol{\mathcal{A}}^\perp_{\mathrm{s},t})_j = -\tfrac{1}{2}(\boldsymbol{n}\times\dot{\boldsymbol{n}})_i, \quad \mathcal{R}_{ij}(\hat{\boldsymbol{z}}\times\boldsymbol{\mathcal{A}}^\perp_{\mathrm{s},t})_j = -\tfrac{1}{2}\dot{\boldsymbol{n}}_i, \quad (24)$$

and $\mathcal{R}_{iz} = n_i$, the induced interface spin density is finally obtained as

$$\boldsymbol{s}^{(\mathrm{N})} = \zeta^{\mathrm{s}}_0\boldsymbol{n} + \mathrm{Re}[\zeta^{\mathrm{s}}](\boldsymbol{n}\times\dot{\boldsymbol{n}}) + \mathrm{Im}[\zeta^{\mathrm{s}}]\dot{\boldsymbol{n}}, \quad (25)$$

where

$$\zeta^{\mathrm{s}}_0 \equiv \frac{1}{2}\sum_\sigma \nu_\sigma T_{\sigma\sigma}, \quad \zeta^{\mathrm{s}} \equiv \frac{\nu_\uparrow - \nu_\downarrow}{2M}T_{\uparrow\downarrow}. \quad (26)$$

Since the N electrons contributing to induced spin density are those at the Fermi energy, the spin current is simply proportional to the induced spin density as $\boldsymbol{j}_{\mathrm{s}}{}^{\mathrm{N}} = \frac{k_F}{m}\boldsymbol{s}^{(\mathrm{N})}$, resulting in

$$\boldsymbol{j}^{(\mathrm{N})}_{\mathrm{s}} = \frac{k_F}{m}\zeta^{\mathrm{s}}_0\boldsymbol{n} + \frac{k_F}{m}\mathrm{Re}[\zeta^{\mathrm{s}}](\boldsymbol{n}\times\dot{\boldsymbol{n}}) + \frac{k_F}{m}\mathrm{Im}[\zeta^{\mathrm{s}}]\dot{\boldsymbol{n}}. \quad (27)$$

This is the result of spin current at the interface. The pumping efficiency is determined by the product of hopping amplitudes $t_\uparrow$ and $t^*_\downarrow$. The spin mixing conductance defined in Ref. [2] corresponds to $T_{\uparrow\downarrow}$. In the scattering approach [2] based on adiabatic pumping theory [3–5], the expression for the spin mixing conductance in terms of scattering matrix element is exact as for the adiabatic contribution. Our result (27), in contrast, is a perturbative one valid to the second order in the hopping amplitude. To take full account of the hopping in the self-energy is possible numerically in a field theoretical approach.

In bulk systems without spin-orbit interaction and magnetic field, the hopping amplitudes t_σ are chosen as real, while at interfaces, this is not the case because inversion symmetry is broken. Nevertheless, in metallic junctions such as Cu/Co, Cr/Fe, and Au/Fe, first-principles calculations indicate that the imaginary part of spin mixing conductance (our ζ^{s}) is smaller than the real part by 1–2 orders of magnitude [22,23]. A large spin current proportional to $\dot{\boldsymbol{n}}$ would therefore suggest existence of strong interface spin-orbit interaction, as shall be discussed in Sec. III.

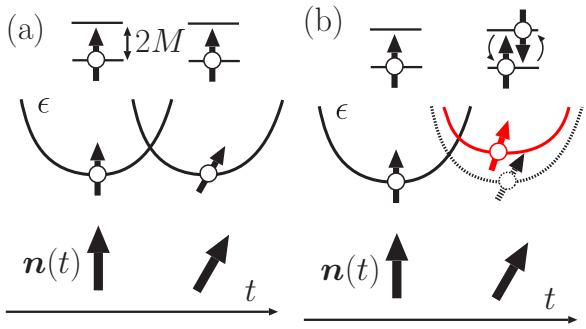

FIG. 4. Schematic figures of electron energy ϵ under precessing localized spin $\boldsymbol{n}(t)$ in the adiabatic limit (a) and with nonadiabaticity (b). Top figures represent energy levels with separation of $2M$ in the rotated frame. In the perfectly adiabatic case (a), the electron state keeps the minimum energy state as $\boldsymbol{n}(t)$ changes. Spin pumping does not occur in this limit. Case (b) is with nonadiabaticity taken into account, where temporal change of localized spin $\dot{\boldsymbol{n}}$ induces a perpendicular spin polarization along $\boldsymbol{n}\times\dot{\boldsymbol{n}}$. This nonadiabatic effect is represented by the nonadiabatic gauge field $\mathcal{A}^\pm_{\mathrm{s},t}$ and causes spin flip in the rotated frame, leading to a high-energy state (shown in red) and spin current generation.

C. Adiabatic or nonadiabatic?

In our approach, the spin pumping effect at the linear order in time derivative is mapped to a static problem of spin polarization formed by a static spin-mixing potential in the rotated frame as was mentioned in Ref. [16]. The rotated-frame approach employed here provides a clear physical picture, as it grasps the low-energy dynamics in a mathematically proper manner. In this approach, it is clearly seen that pumping of spin current arises as a result of off-diagonal components of the spin gauge field that causes electron spin flip.

If so, is spin pumping an adiabatic effect or nonadiabatic one? Conventional adiabatic processes are those where the system under a time-dependent external field remains to be the lowest energy state at each time [Fig. 4(a)]. In the spintronics context, an electron passing through a thick domain wall seems to be in the adiabatic limit in this sense; the electron spin keeps the lowest energy state by rotating it according to the magnetization profile at each spatial point [7] (see Table I). In contrast, as is seen from the above analysis, the spin pumping effect does not arise in the same adiabatic limit; it is induced by the nonadiabatic (off-diagonal) spin gauge field $\mathcal{A}^\pm_{\mathrm{s},t}$, which changes electron spin state in the local rotated frame with a cost of sd exchange energy [Fig. 4(b)]. For the spin pumping effect, therefore, nonadiabaticity is essential, as indicated also in a recent full counting statistics analysis [24].

In spite of this fact, the spin pumping effect appears to be treated within an adiabatic pumping theory [3–5]. In fact, a nonadiabatic gauge field serves just as a driving field for spin current, while the pumping efficiency is determined solely by

TABLE I. Comparison of electron transmission through a domain wall and spin pumping effect. In the figures, large arrows represent the localized spins, $\boldsymbol{n}$, as a function of position x or time t, and the electron spin is denoted by a small arrow with a circle. A nonadiabatic spin polarization $\delta\boldsymbol{s}$ induced by the nonadiabatic gauge field $\mathcal{A}^{\pm}_{\mathrm{s},\mu}$ is essential in both cases (represented by yellow arrows).

	Transmission through domain wall	Magnetization precession
	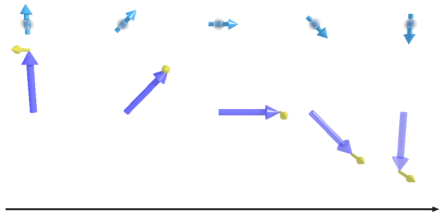	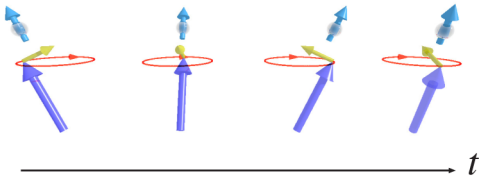
$\delta\boldsymbol{s}$	$\boldsymbol{n}\times\nabla_x\boldsymbol{n}\propto\mathcal{R}\mathcal{A}^{\pm}_{\mathrm{s},x}$	$\boldsymbol{n}\times\dot{\boldsymbol{n}}\propto\mathcal{R}\mathcal{A}^{\pm}_{\mathrm{s},t}$
	Spin-transfer	Spin pumping (FN interface)

the static (adiabatic) response of the system. This feature is the same as the linear response theory; the response function to an external field can be calculated within an equilibrium scheme, although the system is out of equilibrium as a result of the external field. Such separation of a driving field and a response function is possible only by a microscopic formulation, and has not been clearly identified in theories so far.

A careful microscopic description indicates that a nonadiabaticity is essential even in the spin transfer effect. In fact, an electron spin injected into a domain wall along x direction gets polarized along $\boldsymbol{n}\times\nabla_x\boldsymbol{n}$ as a result of a nonadiabatic gauge field [7,25]. This nonequilibrium spin polarization is perpendicular to the wall plane, and thus induces a translational motion of the wall. This is the physical mechanism of spin transfer effect. At the same time, the spin transfer effect can be discussed phenomenologically using the conservation law of angular momentum [26]. One should not forget, however, that nonadiabaticity is implicitly assumed because spin rotation is caused only by a perpendicular component. Physically, the spin pumping effect is essentially the same as electron transmission through the domain wall if we replace a spatial coordinate x and the time, as summarized in Table I. In the case of a domain wall, including the nonadiabatic gauge field to the next order leads to consideration of domain wall resistance and nonadiabatic β torque [27–29], while such a nonadiabatic regime has not been explored in the context of pumping.

III. EFFECTS OF INTERFACE SPIN-ORBIT INTERACTION

In this section, we discuss the effect of spin-orbit interaction at the interface, which modifies hopping amplitude $\tilde{t}_\sigma$. We particularly focus on that linear in the wave vector, namely the interaction represented in the continuum representation by a Hamiltonian

$$H_{\mathrm{so}}=a^2\delta(x)\sum_{ij}\gamma_{ij}k_i\sigma_j, \tag{28}$$

where γ_{ij} is a coefficient having the unit of energy representing the spin-orbit interaction, a is the lattice constant, and the interface is chosen as at $x=0$. Assuming that spin-orbit interaction is weaker than the sd exchange interaction in F, we carry out a unitary transformation to diagonalize the sd interaction to obtain

$$H_{\mathrm{so}}=a^2\delta(x)\sum_{ij}\tilde{\gamma}_{ij}k_i\sigma_j, \tag{29}$$

where $\tilde{\gamma}_{ij}\equiv\sum_l\gamma_{il}\mathcal{R}_{lj}$, with $\mathcal{R}_{ij}$ being a rotation matrix defined by Eq. (22). This spin-orbit interaction modifies the diagonal hopping amplitude $\tilde{t}_i$ in the direction i at the interface to become a complex as

$$\tilde{t}_i=\tilde{t}_i^0-i\sum_j\tilde{\gamma}_{ij}\sigma_j. \tag{30}$$

(In this section, we denote the total hopping amplitude including the interface spin-orbit interaction by $\tilde{t}$ and the one without by $\tilde{t}^0$.) We consider the hopping amplitude perpendicular to the interface, i.e., along the x direction, and suppress the suffix i representing the direction. In the matrix representation for spin, the hopping amplitude is

$$\tilde{t}(\equiv\tilde{t}_x)=\begin{pmatrix}\tilde{t}_\uparrow & \tilde{t}_{\uparrow\downarrow}\\ \tilde{t}_{\downarrow\uparrow} & \tilde{t}_\downarrow\end{pmatrix}, \tag{31}$$

where

$$\begin{aligned}&\tilde{t}_\uparrow=\tilde{t}_\uparrow^0-i\tilde{\gamma}_{xz},\quad \tilde{t}_\downarrow=\tilde{t}_\downarrow^0+i\tilde{\gamma}_{xz},\\ &\tilde{t}_{\uparrow\downarrow}=i(\tilde{\gamma}_{xx}+i\tilde{\gamma}_{xy}),\quad \tilde{t}_{\downarrow\uparrow}=i(\tilde{\gamma}_{xx}-i\tilde{\gamma}_{xy}).\end{aligned} \tag{32}$$

Let us discuss how the spin pumping effect discussed in Sec. II B is modified when the hopping amplitude is a matrix of Eq. (31). The spin pumping efficiency is written as in Eqs. (21) and (26). In the absence of spin-orbit interaction, the hopping amplitude $\tilde{t}$ is chosen as real, and thus the contribution proportional to $\boldsymbol{n}\times\dot{\boldsymbol{n}}$ in Eq. (27) is dominant. The spin-orbit interaction enhances the other contribution proportional to $\dot{\boldsymbol{n}}$ because it gives rise to an imaginary part. Moreover, it leads to spin mixing at the interface, modifying the spin accumulation formed in the N region at the interface.

The electron states in the N region at the interface are now given instead of Eq. (18) by the following two states (choosing the basis as $\binom{|k_F\uparrow\rangle}{|k_F\downarrow\rangle}$):

$$|k_{\rm F}\uparrow\rangle_{\rm N} \equiv \widetilde{t}|k_{\rm F\uparrow}\uparrow\rangle_{\rm F} = \begin{pmatrix} \widetilde{t}_\uparrow - \widetilde{t}_{\uparrow\downarrow}\frac{\mathcal{A}^+_{{\rm s},t}}{M} \\ \widetilde{t}_{\downarrow\uparrow} - \widetilde{t}_\downarrow \frac{\mathcal{A}^+_{{\rm s},t}}{M} \end{pmatrix},$$
$$|k_{\rm F}\downarrow\rangle_{\rm N} \equiv \widetilde{t}|k_{\rm F\downarrow}\downarrow\rangle_{\rm F} = \begin{pmatrix} \widetilde{t}_{\uparrow\downarrow} + \widetilde{t}_\uparrow \frac{\mathcal{A}^-_{{\rm s},t}}{M} \\ \widetilde{t}_\downarrow + \widetilde{t}_{\downarrow\uparrow}\frac{\mathcal{A}^-_{{\rm s},t}}{M} \end{pmatrix}. \tag{33}$$

The pumped (i.e., linear in the gauge field) spin density for these two states are

$$\begin{aligned} {}_{\rm N}\langle k_F\uparrow|\boldsymbol{\sigma}|k_F\uparrow\rangle_{\rm N} = -\frac{2}{M}\Bigg(& \boldsymbol{\mathcal{A}}^\perp_{{\rm s},t}{\rm Re}[T^{\rm tot}_{\uparrow\downarrow}] + (\hat{\boldsymbol{z}}\times\boldsymbol{\mathcal{A}}^\perp_{{\rm s},t}){\rm Im}[T^{\rm tot}_{\uparrow\downarrow}] \\ & + {\rm Re}[(\widetilde{t}_{\uparrow\downarrow})^*\widetilde{t}_{\downarrow\uparrow}]\begin{pmatrix} \mathcal{A}^x_{{\rm s},t} \\ -\mathcal{A}^y_{{\rm s},t} \\ 0 \end{pmatrix} \\ & + {\rm Im}[(\widetilde{t}_{\uparrow\downarrow})^*\widetilde{t}_{\downarrow\uparrow}]\begin{pmatrix} \mathcal{A}^y_{{\rm s},t} \\ \mathcal{A}^x_{{\rm s},t} \\ 0 \end{pmatrix}\Bigg) \\ & - \hat{\boldsymbol{z}}\big(\mathcal{A}^x_{{\rm s},t}{\rm Re}[(\widetilde{t}_\uparrow)^*\widetilde{t}_{\uparrow\downarrow} - \widetilde{t}_\downarrow(\widetilde{t}_{\downarrow\uparrow})^*] \\ & - \mathcal{A}^y_{{\rm s},t}{\rm Im}[(\widetilde{t}_\uparrow)^*\widetilde{t}_{\uparrow\downarrow} - \widetilde{t}_\downarrow(\widetilde{t}_{\downarrow\uparrow})^*]\big), \end{aligned} \tag{34}$$

$$\begin{aligned} {}_{\rm N}\langle k_F\downarrow|\boldsymbol{\sigma}|k_F\downarrow\rangle_{\rm N} = \frac{2}{M}\Bigg(& \boldsymbol{\mathcal{A}}^\perp_{{\rm s},t}{\rm Re}[T^{\rm tot}_{\uparrow\downarrow}] + (\hat{\boldsymbol{z}}\times\boldsymbol{\mathcal{A}}^\perp_{{\rm s},t}){\rm Im}[T^{\rm tot}_{\uparrow\downarrow}] \\ & + {\rm Re}[(\widetilde{t}_{\uparrow\downarrow})^*\widetilde{t}_{\downarrow\uparrow}]\begin{pmatrix} \mathcal{A}^x_{{\rm s},t} \\ -\mathcal{A}^y_{{\rm s},t} \\ 0 \end{pmatrix} \\ & + {\rm Im}[(\widetilde{t}_{\uparrow\downarrow})^*\widetilde{t}_{\downarrow\uparrow}]\begin{pmatrix} \mathcal{A}^y_{{\rm s},t} \\ \mathcal{A}^x_{{\rm s},t} \\ 0 \end{pmatrix}\Bigg) \\ & + \hat{\boldsymbol{z}}\big(\mathcal{A}^x_{{\rm s},t}{\rm Re}[(\widetilde{t}_\uparrow)^*\widetilde{t}_{\uparrow\downarrow} - \widetilde{t}_\downarrow(\widetilde{t}_{\downarrow\uparrow})^*] \\ & - \mathcal{A}^y_{{\rm s},t}{\rm Im}[(\widetilde{t}_\uparrow)^*\widetilde{t}_{\uparrow\downarrow} - \widetilde{t}_\downarrow(\widetilde{t}_{\downarrow\uparrow})^*]\big). \end{aligned} \tag{35}$$

We here focus on the linear effect of interface spin-orbit interaction and neglect the spin polarization along the magnetization direction, $\boldsymbol{n}$. The expression for the pumped spin current then agrees with Eq. (27) with the amplitude $\zeta^{\rm s}$ written in terms of hopping including the interface spin orbit,

$$T_{\uparrow\downarrow} = ((\tilde{t}^0_\uparrow)^* + i(\widetilde{\gamma}_{xz})^*)(\tilde{t}^0_\downarrow + i\widetilde{\gamma}_{xz}). \tag{36}$$

In metallic junctions of Cu/Co, Cr/Fe, and Au/Fe, ${\rm Im}[T_{\uparrow\downarrow}]$ is orders of magnitude smaller than ${\rm Re}[T_{\uparrow\downarrow}]$ [22,23], suggesting that the imaginary part of bare hopping amplitude $\tilde{t}^0_\sigma$ is small. According to Eq. (36), large ${\rm Im}[T_{\uparrow\downarrow}]$ is expected if strong interface spin-orbit interaction exist. If the imaginary part of $\tilde{t}^0_\sigma$ is neglected, we obtain (using $\widetilde{\gamma}_{xz} = n_i\gamma_{xi}$)

$${\rm Im}[\zeta^{\rm s}] = \frac{\nu_\uparrow - \nu_\downarrow}{2M}(\tilde{t}^0_\uparrow + \tilde{t}^0_\downarrow)\gamma_{xi}n_i. \tag{37}$$

The measurement of the amplitude of the spin current is proportional to $\dot{\boldsymbol{n}}$, thus, it works as a probe for the interface spin-orbit interaction strength γ_{xi}.

Let us discuss some examples. Of recent particular interest is the interface Rashba interaction, represented by the anti-symmetric coefficient

$$\gamma^{\rm (R)}_{ij} = \epsilon_{ijk}\alpha^{\rm R}_k, \tag{38}$$

where $\boldsymbol{\alpha}^{\rm R}$ is a vector representing the Rashba field. In the case of an interface, $\boldsymbol{\alpha}^{\rm R}$ is perpendicular to the interface, i.e., $\boldsymbol{\alpha}^{\rm R} \parallel \hat{\boldsymbol{x}}$. Therefore the interface Rashba interaction leads to $\gamma^{\rm (R)}_{xj} = 0$ and does not modify the spin pumping effect at the linear order. (It contributes at the second order as discussed in Ref. [15].) In other words, the vector coupling between the wave vector and spin in the form of $\boldsymbol{k}\times\boldsymbol{\sigma}$ exists only along the x direction, and does not affect the interface hopping (i.e., does not include k_x).

In contrast, a scalar coupling $\eta^{\rm (D)}(\boldsymbol{k}\cdot\boldsymbol{\sigma})$ ($\eta^{\rm (D)}$ is a coefficient), called the Dirac type spin-orbit interaction, leads to $\gamma^{\rm (D)}_{ij} = \eta^{\rm (D)}\delta_{ij}$. The spin current along $\dot{\boldsymbol{n}}$ then reads

$$\boldsymbol{j}^{\dot{\boldsymbol{n}}}_{\rm s} = \eta^{\rm (D)}\frac{k_F(\nu_\uparrow - \nu_\downarrow)}{2mM}(\tilde{t}^0_\uparrow + \tilde{t}^0_\downarrow)n_x\dot{\boldsymbol{n}}. \tag{39}$$

For the case of in-plane easy axis along the z direction and magnetization precession given by $\boldsymbol{n}(t) = (\sin\theta\cos\omega t, \sin\theta\sin\omega t, \cos\theta)$, where θ is the precession angle and ω is the angular frequency, we expect to have a dc spin current along the y direction, as $\overline{n_x\dot{\boldsymbol{n}}} = -\frac{\omega}{2}\sin^2\theta\,\hat{\boldsymbol{y}}$ ($\overline{n_x\dot{\boldsymbol{n}}}$ denotes time average).

Recently, spin pumping effects are discussed including a phenomenological "spin-memory loss" parameter $\delta_{\rm sml}$, to represent the interface spin-flip rate [30,31]. The parameter corresponds roughly to $\delta_{\rm sml} = |\widetilde{t}_{\uparrow\downarrow}|^2/(|\widetilde{t}_\uparrow|^2 + |\widetilde{t}_\downarrow|^2)$ in our scheme [see Eq. (31)].

IV. FIELD THEORETIC DESCRIPTION OF METALLIC CASE

Here we present a field-theoretic description of the spin pumping effect of a metallic ferromagnet. The many-body approach has an advantage of taking into account the particle distributions automatically. Moreover, it describes the propagation of particle density in terms of the Green's functions, and thus is suitable for studying spatial propagation as well as for intuitive understanding of transport phenomena. All the transport coefficients are determined by material constants.

The formalism presented here is essentially the same as in Ref. [16], but treats ferromagnets of finite size and takes account of electron states with different wave vectors. Interface spin-orbit interaction is not considered here.

Conduction electrons in ferromagnetic and normal metals are denoted by field operators d, $d^\dagger$ and c, $c^\dagger$, respectively. These operators are vectors with two spin components, i.e., $d \equiv (d_\uparrow, d_\downarrow)$. The Hamiltonian describing the F and N electrons

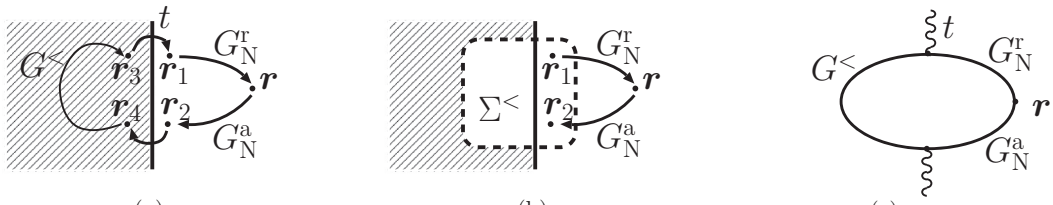

FIG. 5. (a) Schematic diagrammatic representations of the lesser Green's function for an N electron connecting the same position $\boldsymbol{r}$, $G^<_{\rm N}(\boldsymbol{r},\boldsymbol{r}) \simeq G^{\rm r}_{\rm N}\Sigma^<_{\rm N}G^{\rm a}_{\rm N}$ representing the propagation of electron density. It is decomposed into a propagation of N electrons from $\boldsymbol{r}$ to the interface at $\boldsymbol{r}_2$, then hopping to $\boldsymbol{r}_4$ in the F side, a propagation inside F, followed by a hopping to N side (to $\boldsymbol{r}_1$) and propagation back to $\boldsymbol{r}$. [Position labels are as in Eqs. (43) and (44).] (b): The self-energy $\Sigma^<_{\rm N}$ represents all the effects of the ferromagnet. (c) Standard Feynman diagram representation of lesser Green's function for N at $\boldsymbol{r}$, Eqs. (46) and (44).

is $H_{\rm F}+H_{\rm N}$, where

$$H_{\rm F} \equiv \int_{\rm F} d^3r d^\dagger\left(-\frac{\nabla^2}{2m}-\epsilon_F - M\boldsymbol{n}(t)\cdot\boldsymbol{\sigma}\right)d,$$
$$H_{\rm N} \equiv \int_{\rm N} d^3r c^\dagger\left(-\frac{\nabla^2}{2m}-\epsilon_F\right)c. \tag{40}$$

We set the Fermi energies for the ferromagnet and the normal metal equal. The hopping through the interface is described by the Hamiltonian

$$H_{\rm I} \equiv \int_{\rm I_F} d^3r \int_{\rm I_N} d^3\boldsymbol{r}'(c^\dagger(\boldsymbol{r}')t(\boldsymbol{r}',\boldsymbol{r},t)d(\boldsymbol{r}) + d^\dagger(\boldsymbol{r})t^*(\boldsymbol{r}',\boldsymbol{r},t)c(\boldsymbol{r}')), \tag{41}$$

where $t(\boldsymbol{r}',\boldsymbol{r},t)$ represents the hopping amplitude of electrons from $\boldsymbol{r}$ in the ferromagnetic regime to a site $\boldsymbol{r}'$ in the normal region and the integrals are over the interface (denoted by $\rm I_F$ and $\rm I_N$ for F and N regions, respectively). The hopping amplitude is generally a matrix that depends on the magnetization direction $\boldsymbol{n}(t)$, and thus depends on time t. Hopping is treated as energy conserving. Assuming a sharp interface at $x=0$, the momentum perpendicular to the interface is not conserved on hopping.

We are interested in the spin current in the normal region, given by

$$j^\alpha_{{\rm s},i}(\boldsymbol{r},t) = -\frac{1}{4m}(\nabla^{(\boldsymbol{r})}-\nabla^{(\boldsymbol{r}')})_i{\rm tr}[\sigma_\alpha G^<_{\rm N}(\boldsymbol{r},t,\boldsymbol{r}',t)|_{\boldsymbol{r}'=\boldsymbol{r}}, \tag{42}$$

where $G^<_{\rm N}(\boldsymbol{r},t,\boldsymbol{r}',t') \equiv i\langle c(\boldsymbol{r},t)c^\dagger(\boldsymbol{r}',t')\rangle$ denotes the lesser Green's function for the normal region. It is calculated from the Dyson's equation for the path-ordered Green's function defined for a complex time along a complex contour C:

$$G_{\rm N}(\boldsymbol{r},t,\boldsymbol{r}',t') = g_{\rm N}(\boldsymbol{r}-\boldsymbol{r}',t-t') + \int_c dt_1\int_c dt_2\int d^3r_1 \times\int d^3r_2 g_{\rm N}(\boldsymbol{r}-\boldsymbol{r}_1,t-t_1) \times\Sigma_{\rm N}(\boldsymbol{r}_1,t_1,\boldsymbol{r}_2,t_2)G_{\rm N}(\boldsymbol{r}_2,t_2,\boldsymbol{r}',t'), \tag{43}$$

where $g^<_{\rm N}$ denotes the Green's function without interface hopping and $\Sigma_{\rm N}(\boldsymbol{r}_1,t_1,\boldsymbol{r}_2,t_2)$ is the self-energy for N electrons, given by the contour-ordered Green's function in the ferromagnet as

$$\Sigma_{\rm N}(\boldsymbol{r}_1,t_1,\boldsymbol{r}_2,t_2) \equiv \int_{\rm I_F} d^3r_3\int_{\rm I_F} d^3r_4 t(\boldsymbol{r}_1,\boldsymbol{r}_3,t_1) \times G(\boldsymbol{r}_3,t_1,\boldsymbol{r}_4,t_2)t^*(\boldsymbol{r}_2,\boldsymbol{r}_4,t_2). \tag{44}$$

Here, $\boldsymbol{r}_1$ and $\boldsymbol{r}_2$ are coordinates at the interface $\rm I_N$ in N region and $\boldsymbol{r}_3$ and $\boldsymbol{r}_4$ are those in $\rm I_F$ for F. G is the contour-ordered Green's function for F electrons in the laboratory frame including the effect of spin gauge field. We denote the Green's functions of F electrons by G and g without suffix and those of N electrons with suffix N. The lesser component of the normal metal Green's function is obtained from Eq. (43) as (suppressing the time and space coordinates)

$$G^<_{\rm N} = \left(1+G^{\rm r}_{\rm N}\Sigma^{\rm r}_{\rm N}\right)g^<_{\rm N}\left(1+\Sigma^{\rm a}_{\rm N}G^{\rm a}_{\rm N}\right) + G^{\rm r}_{\rm N}\Sigma^<_{\rm N}G^{\rm a}_{\rm N}. \tag{45}$$

For pumping effects, the last term on the right-hand side is essential, as it contains the information of excitations in F region [16]. We thus consider the second term only,

$$G^<_{\rm N} \simeq G^{\rm r}_{\rm N}\Sigma^<_{\rm N}G^{\rm a}_{\rm N}, \tag{46}$$

and neglect the spin dependence of the normal region Green's functions, $G^{\rm r}_{\rm N}$ and $G^{\rm a}_{\rm N}$. The contribution is diagrammatically shown in Fig. 5.

A. Rotated frame

To solve for the Green's function in the ferromagnet, it is convenient to use the rotated frame we used in Sec. II A. In the field representation, the unitary transformation is represented as [Fig. 6(c)]

$$d = U\tilde{d}, \quad c = U\tilde{c}, \tag{47}$$

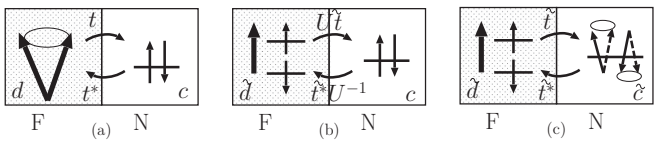

FIG. 6. Unitary transformation U of F electrons converts the original system with field operator d [shown as (a)] to the rotated one with field operator $\tilde{d} \equiv U^{-1}d$ (b). The hopping amplitude for representation in (b) is modified by U. If N electrons are also rotated as $\tilde{c} \equiv U^{-1}c$, hopping becomes $\tilde{t} \equiv U^{-1}tU$, while the N electron spin rotates with time, as shown as (c).

where U is the same 2×2 matrix defined in Eq. (10). We rotate N electrons as well as F electrons, to simplify the following expressions. The hopping interaction Hamiltonian reads

$$H_{\rm I}=\int_{\rm I_F}d^3r\int_{\rm I_N}d^3r'(\tilde{c}^\dagger(\boldsymbol{r}')\tilde{t}(\boldsymbol{r}',\boldsymbol{r})\tilde{d}(\boldsymbol{r}) + \tilde{d}^\dagger(\boldsymbol{r})\tilde{t}^*(\boldsymbol{r}',\boldsymbol{r})\tilde{c}(\boldsymbol{r}')), \tag{48}$$

where

$$\tilde{t}(\boldsymbol{r}',\boldsymbol{r})\equiv U^\dagger(t)t(\boldsymbol{r}',\boldsymbol{r},t)U(t) \tag{49}$$

is the hopping amplitude in the rotated frame. The rotated amplitude (neglecting interface spin-orbit interaction) is diagonal in spin:

$$\tilde{t}=\begin{pmatrix}\tilde{t}_\uparrow & 0\\ 0 & \tilde{t}_\downarrow\end{pmatrix}. \tag{50}$$

Including the interaction with a spin gauge field, the Hamiltonian for F and N electrons in the momentum representation is

$$H_{\rm F}+H_{\rm N}=\sum_{\boldsymbol{k}}\tilde{d}^\dagger_{\boldsymbol{k}}\begin{pmatrix}\epsilon_k-M-\mathcal{A}^z_{{\rm s},t} & \mathcal{A}^-_{{\rm s},t}\\ \mathcal{A}^+_{{\rm s},t} & \epsilon_k+M+\mathcal{A}^z_{{\rm s},t}\end{pmatrix}\tilde{d}_{\boldsymbol{k}} + \sum_{\boldsymbol{k}}\epsilon^{\rm (N)}_{\boldsymbol{k}}\tilde{c}^\dagger_{\boldsymbol{k}}\tilde{c}_{\boldsymbol{k}}. \tag{51}$$

As for the hopping, we consider the case the interface is atomically sharp. The hopping Hamiltonian is then written in the momentum space as

$$H_{\rm I}=\sum_{\boldsymbol{k}\boldsymbol{k}'}(\tilde{c}^\dagger(\boldsymbol{k})\tilde{t}(\boldsymbol{k},\boldsymbol{k}')\tilde{d}(\boldsymbol{k}')+\tilde{d}^\dagger(\boldsymbol{k}')\tilde{t}^*(\boldsymbol{k},\boldsymbol{k}')\tilde{c}(\boldsymbol{k})), \tag{52}$$

where $\boldsymbol{k}=(k_x,k_y,k_z)$, $\boldsymbol{k}'=(k'_x,k_y,k_z)$, choosing the interface as the plane of $x=0$. Namely, the wave vectors parallel to the interface are conserved while k_x and k'_x are uncorrelated.

B. Spin polarization and current in N

Pumped spin current in N is calculated by using Eqs. (42) and (46). The lesser component of the self-energy connecting Green's functions with wave vectors $\boldsymbol{k}$ and $\boldsymbol{k}'$ is written using Eq. (44) as (in the matrix notation)

$$\Sigma^<_{\rm N}(\boldsymbol{k},\boldsymbol{k}')=\sum_{\boldsymbol{k}''}\tilde{t}(\boldsymbol{k},\boldsymbol{k}'')G^<(\boldsymbol{k}'')\tilde{t}^*(\boldsymbol{k}'',\boldsymbol{k}'). \tag{53}$$

The lesser Green's function in F in the rotated frame is calculated including the spin gauge field (a driving field of spin pumping) to the linear order by use of the Dyson's equation

$$G^<=g^<+g^{\rm r}(\boldsymbol{\mathcal{A}}_{{\rm s},t}\cdot\boldsymbol{\sigma})g^<+g^<(\boldsymbol{\mathcal{A}}_{{\rm s},t}\cdot\boldsymbol{\sigma})g^{\rm a}, \tag{54}$$

where g^α ($\alpha=<,{\rm r},{\rm a}$) represents Green's functions without a spin gauge field. The lesser Green's function satisfies for static case $g^<=F(g^{\rm a}-g^{\rm r})$, where $F\equiv\left(\begin{smallmatrix}f_\uparrow & 0\\ 0 & f_\downarrow\end{smallmatrix}\right)$ is the spin-dependent Fermi distribution function. We thus obtain the Green's function at the linear order, written as $\delta G^<$, as [16]

$$\delta G^<=g^{\rm r}[\boldsymbol{\mathcal{A}}_{{\rm s},t}\cdot\boldsymbol{\sigma},F]g^{\rm a}+g^{\rm a}F(\boldsymbol{\mathcal{A}}_{{\rm s},t}\cdot\boldsymbol{\sigma})g^{\rm a} - g^{\rm r}(\boldsymbol{\mathcal{A}}_{{\rm s},t}\cdot\boldsymbol{\sigma})Fg^{\rm r}. \tag{55}$$

The last two terms of the right-hand side are rapidly oscillating as a function of position and are neglected. The commutator is calculated as (sign $\pm$ denotes spin $\uparrow$ and $\downarrow$)

$$[\boldsymbol{\mathcal{A}}_{{\rm s},t}\cdot\boldsymbol{\sigma},F]=(f_+-f_-)\sum_\pm(\pm)\mathcal{A}^\pm_{{\rm s},t}\sigma_\mp. \tag{56}$$

The self-energy linear in the spin gauge field is thus

$$\Sigma^<_{\rm N}(\boldsymbol{k},\boldsymbol{k}')=\sum_\pm\sigma_\mp\sum_{\boldsymbol{k}''}(f_{\boldsymbol{k}''\pm}-f_{\boldsymbol{k}''\mp})\mathcal{A}^\pm_{{\rm s},t}\tilde{t}_\mp(\boldsymbol{k},\boldsymbol{k}'') \times\tilde{t}^*_\pm(\boldsymbol{k}'',\boldsymbol{k}')g^{\rm r}_\mp(\boldsymbol{k}'',\omega)g^{\rm a}_\pm(\boldsymbol{k}'',\omega). \tag{57}$$

The spin polarization of an N electron therefore reads (diagram shown in Fig. 7)

$$-i{\rm tr}[\sigma_\pm G^<_{\rm N}(\boldsymbol{r},t,\boldsymbol{r}',t)] = -i\sum_{\boldsymbol{k}\boldsymbol{k}'\boldsymbol{k}''}e^{i\boldsymbol{k}\cdot\boldsymbol{r}}e^{-i\boldsymbol{k}'\cdot\boldsymbol{r}'}g^{\rm r}_{\rm N}(\boldsymbol{k},\omega)g^{\rm a}_{\rm N}(\boldsymbol{k}',\omega)(f_{\boldsymbol{k}''\pm}-f_{\boldsymbol{k}''\mp}) \times\mathcal{A}^\pm_{{\rm s},t}\tilde{t}_\mp(\boldsymbol{k},\boldsymbol{k}'')\tilde{t}^*_\pm(\boldsymbol{k}'',\boldsymbol{k}')g^{\rm r}_\mp(\boldsymbol{k}'',\omega)g^{\rm a}_\pm(\boldsymbol{k}'',\omega). \tag{58}$$

We assume that the dependence of N Green's functions on ω is weak and use $\sum_{\boldsymbol{k}}e^{i\boldsymbol{k}\cdot\boldsymbol{r}}g^{\rm r}_{\rm N}(\boldsymbol{k},\omega)=-i\pi\nu_{\rm N}e^{ik_Fx}e^{-|x|/\ell}\equiv g^{\rm r}_{\rm N}(\boldsymbol{r})$, where ℓ is the elastic mean free path, $\nu_{\rm N}$ and k_F are the density of states at the Fermi energy and Fermi wave vector, respectively, whose ω dependencies are neglected. (For an infinitely wide interface, the Green's function becomes one dimensional.) As a result of summation over wave vectors, the product of hopping amplitudes $\tilde{t}_\mp(\boldsymbol{k},\boldsymbol{k}'')\tilde{t}^*_\pm(\boldsymbol{k}'',\boldsymbol{k}')$ is replaced by the average over the Fermi surface, $\overline{\tilde{t}_\mp\tilde{t}^*_\pm}\equiv\overline{T_{\pm\mp}}$, i.e.,

$$\tilde{t}_\mp(\boldsymbol{k},\boldsymbol{k}'')\tilde{t}^*_\pm(\boldsymbol{k}'',\boldsymbol{k}')\to\overline{T_{\pm\mp}}. \tag{59}$$

The spin polarization of N electrons induced by magnetization dynamics (the spin gauge field) is therefore obtained in the rotated frame as [with correlation function $\chi_\pm$ defined in Eq. (A5)]

$$\tilde{s}^{\rm (N)}_\pm(\boldsymbol{r},t)=-\left|g^{\rm r}_{\rm N}(\boldsymbol{r})\right|^2\sum_\pm\mathcal{A}^\pm_{{\rm s},t}\chi_\pm\overline{T_{\pm\mp}}, \tag{60}$$

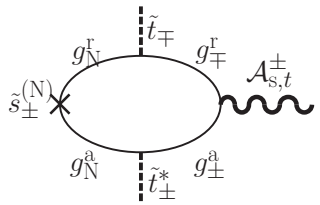

FIG. 7. Feynman diagram for electron spin density of normal metal driven by the spin gauge field of ferromagnetic metal $\mathcal{A}_{\rm s}$. The spin current is represented by the same diagram but with spin current vertex.

or using $\chi_+^* = \chi_-$,

$$\tilde{\boldsymbol{s}}^{(\mathrm{N})}(\boldsymbol{r},t) = -2\left|g_{\mathrm{N}}^{\mathrm{r}}(\boldsymbol{r})\right|^2[\boldsymbol{\mathcal{A}}_{\mathrm{s},t}^{\perp}\mathrm{Re}[\chi_+\overline{T_{+-}}] + (\hat{\boldsymbol{z}}\times\boldsymbol{\mathcal{A}}_{\mathrm{s},t}^{\perp})\mathrm{Im}[\chi_+\overline{T_{+-}}]]. \tag{61}$$

In the laboratory frame, we have (using $s_i^{(\mathrm{N})} = \mathcal{R}_{ij}\tilde{s}_j^{(\mathrm{N})}$)

$$\boldsymbol{s}^{(\mathrm{N})}(\boldsymbol{r},t) = \left|g_{\mathrm{N}}^{\mathrm{r}}(\boldsymbol{r})\right|^2[\mathrm{Re}[\chi_+\overline{T_{+-}}](\boldsymbol{n}\times\dot{\boldsymbol{n}}) + \mathrm{Im}[\chi_+\overline{T_{+-}}]\dot{\boldsymbol{n}}]. \tag{62}$$

The spin current induced in N region is similarly given by (neglecting the contribution proportional to $\boldsymbol{n}$)

$$\begin{aligned}\boldsymbol{j}_{\mathrm{s}}(\boldsymbol{r},t) &= \frac{k_F}{m}\left|g_{\mathrm{N}}^{\mathrm{r}}(\boldsymbol{r})\right|^2[\mathrm{Re}[\chi_+\overline{T_{+-}}](\boldsymbol{n}\times\dot{\boldsymbol{n}}) + \mathrm{Im}[\chi_+\overline{T_{+-}}]\dot{\boldsymbol{n}}] \\ &= e^{-|x|/\ell}(\mathrm{Re}[\zeta^{\mathrm{s}}](\boldsymbol{n}\times\dot{\boldsymbol{n}}) + \mathrm{Im}[\zeta^{\mathrm{s}}]\dot{\boldsymbol{n}}),\end{aligned} \tag{63}$$

where

$$\zeta^{\mathrm{s}} \equiv \pi^2\frac{k_F\nu_{\mathrm{N}}^2}{2mM}(n_+ - n_-)\overline{T_{+-}}. \tag{64}$$

The coefficient ζ^{s} is essentially the same as the one in Eq. (27) derived by a quantum mechanical argument, as the quantum mechanical dimensionless hopping amplitude corresponds to $\nu_{\mathrm{N}}\tilde{t}$ of the field representation.

For a $3d$ ferromagnet, we may estimate the spin current by approximating roughly $M \sim 1/\nu_{\mathrm{N}} \sim \epsilon_F \sim 1$ eV and $n_\sigma \sim {k_F}^3$. The hopping amplitude $|\overline{T_{+-}}|$ in the metallic case would be of order of ϵ_F. The spin current density then is of the order of (including electric charge e and recovering $\hbar$) $j_{\mathrm{s}} \sim e\frac{\hbar k_F}{m}\frac{\hbar\hbar\omega}{\epsilon_F} \sim 5\times10^{11}$ A/m^2 if the precession frequency is 10 GHz.

V. SPIN ACCUMULATION IN FERROMAGNET

The spin current pumping is equivalent to the increase of spin damping due to magnetization precession, as was discussed in Refs. [2,11]. In this section, we confirm this fact by calculating the torque by evaluating the spin polarization of the conduction electron spin in F region. (The spin accumulation without taking into account an interface is calculated in Appendix A.)

There are several ways to evaluate the damping of magnetization. One way is to calculate the spin-flip probability of the electron as in Ref. [11], which leads to damping of localized spin in the presence of strong sd exchange interaction. The second is to estimate the torque on the electron by use of the equation of motion [32]. The relation between the damping and spin current generation is clearly seen in this approach. In fact, the total torque acting on conduction electrons is ($\hbar$ times) the time derivative of the electron spin density,

$$\frac{d\boldsymbol{s}}{dt} = i(\langle[H,d^\dagger]\boldsymbol{\sigma}d\rangle + \langle d^\dagger\boldsymbol{\sigma}[H,d]\rangle). \tag{65}$$

At the interface, the right-hand side arises from the interface hopping. Using the hopping Hamiltonian of Eq. (41), we have

$$\left.\frac{d\boldsymbol{s}}{dt}\right|_{\mathrm{interface}} = i(\langle c^\dagger t\boldsymbol{\sigma}d\rangle - \langle d^\dagger\boldsymbol{\sigma}t^\dagger c\rangle), \tag{66}$$

as the interface contribution. As is natural, the right-hand side agrees with the definition of the spin current passing through the interface. Evaluating the right-hand side, we obtain in general a term proportional to $\boldsymbol{n}\times\dot{\boldsymbol{n}}$, which gives the Gilbert damping, and a term proportional to $\dot{\boldsymbol{n}}$, which gives a renormalization of the magnetization. In contrast, away from the interface, the commutator $[H,d]$ arises from the kinetic term $H_0 \equiv \int d^3r\frac{|\nabla d|^2}{2m}$ describing electron propagation, resulting in

$$\begin{aligned}\frac{ds_\alpha}{dt} &= i(\langle[H_0,d^\dagger]\boldsymbol{\sigma}d\rangle + \langle d^\dagger\boldsymbol{\sigma}[H,d]\rangle) \\ &= \nabla\cdot\boldsymbol{j}_{\mathrm{s}}^\alpha,\end{aligned} \tag{67}$$

where $\boldsymbol{j}_{\mathrm{s}}^\alpha(\boldsymbol{r}) \equiv \frac{-i}{2m}(\nabla_{\boldsymbol{r}} - \nabla_{\boldsymbol{r}'})\langle d^\dagger(\boldsymbol{r}')\sigma_\alpha d(\boldsymbol{r})\rangle|_{\boldsymbol{r}'=\boldsymbol{r}}$ is the spin current. Away from the interface, the damping therefore occurs if the spin current has a source or a sink at the site of interest.

Here we use the third approach and estimate the torque on the localized spin by calculating the spin polarization of electrons as was done in Refs. [7,33]. The electron spin polarization at position $\boldsymbol{r}$ in the ferromagnet at time t is $\boldsymbol{s}^{(\mathrm{F})}(\boldsymbol{r},t) \equiv \langle d^\dagger\boldsymbol{\sigma}d\rangle$, which reads in the rotated frame $s_\alpha^{(\mathrm{F})} = \mathcal{R}_{\alpha\beta}\tilde{s}_\beta^{(\mathrm{F})}$, where

$$\tilde{s}_\beta^{(\mathrm{F})}(\boldsymbol{r},t) = -i\,\mathrm{tr}[\sigma_\beta G^<(\boldsymbol{r},\boldsymbol{r},t,t)], \tag{68}$$

where $G^<_{\sigma\sigma'}(\boldsymbol{r},\boldsymbol{r}',t,t') \equiv i\langle\tilde{d}^\dagger_{\sigma'}\tilde{d}_\sigma\rangle$ is the lesser Green's function in F region, which is a matrix in spin space ($\sigma,\sigma' = \pm$). We are interested in the effect of the N region arising from the hopping. We must note that the hopping interaction of Eq. (48) is not convenient for integrating out N electrons, since the $\tilde{c}$ electrons' spins are time-dependent as a result of a unitary transformation $U(t)$. We thus use the following form [Fig. 6(b)],

$$\begin{aligned}H_{\mathrm{I}} = \int_{\mathrm{I_F}}d^3r\int_{\mathrm{I_N}}d^3r'(c^\dagger(\boldsymbol{r}')U\tilde{t}(\boldsymbol{r}',\boldsymbol{r})\tilde{d}(\boldsymbol{r}) \\ + \tilde{d}^\dagger(\boldsymbol{r})\tilde{t}^*(\boldsymbol{r}',\boldsymbol{r})U^\dagger c(\boldsymbol{r}')),\end{aligned} \tag{69}$$

namely, the hopping amplitude between $\tilde{d}$ and c electrons includes the unitary matrix U.

Let us briefly argue in the rotated frame why the effect of damping arising from the interface. In the totally rotated frame of Fig. 6(c), the spin of an F electron is static, while that of N electron varies with time. When an F electron hops to N region and comes back, therefore, the electron spin gets rotated with the amount depending on the time it stayed in N region. This effect is in fact represented by a retardation effect of the matrices U and U^{-1} in Eq. (69). If the off-diagonal nature of U and U^{-1} is neglected, the interface effects are all spin-conserving and do not induce damping for F electrons (see Appendix B).

The spin density is calculated by evaluating the lesser Green's function in F. Including the effect of interface in terms of self-energy, it reads

$$G^<(\boldsymbol{r},t,\boldsymbol{r}',t) = g^{\mathrm{r}}\Sigma^{\mathrm{r}}g^{\mathrm{a}} + g^{\mathrm{r}}\Sigma^<g^{\mathrm{a}} + g^<\Sigma^{\mathrm{a}}g^{\mathrm{a}}, \tag{70}$$

where the self-energy of an F electron arising from the hopping to N region reads ($\boldsymbol{r}_1$ and $\boldsymbol{r}_2$ are in F and $a = \mathrm{r,a,<}$)

$$\begin{aligned}\Sigma^a(\boldsymbol{r}_1,\boldsymbol{r}_2,t_1,t_2) = \int_{\mathrm{I_N}}d^3r_1'\int_{\mathrm{I_N}}d^3r_2'\tilde{t}(\boldsymbol{r}_1,\boldsymbol{r}_1')U^{-1}(t_1) \\ \times g_{\mathrm{N}}^a(\boldsymbol{r}_1',\boldsymbol{r}_2',t_1-t_2)U(t_2)\tilde{t}^\dagger(\boldsymbol{r}_2,\boldsymbol{r}_2').\end{aligned} \tag{71}$$

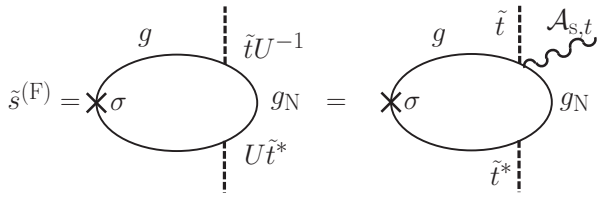

FIG. 8. Diagrammatic representation of the spin accumulation in a ferromagnetic metal induced as a result of coupling to the normal metal [Eqs. (68) and (C1)]. Conduction electron Green's functions in a ferromagnet and normal metal are denoted by g and g_{N}, respectively. Time-dependent matrix $U(t)$, defined by Eq. (10), represents the effect of dynamic magnetization. Expanding U and U^{-1} with respect to the slow time dependence of magnetization, we obtain a gauge field representation, see Eq. (C3).

Expanding to the linear order in the spin gauge field arising from the time dependence of unitary matrix U, we obtain

$$G^{<}(\boldsymbol{r},t,\boldsymbol{r}',t) = 2\pi i \nu_{\mathrm{N}} a^2 \int \frac{d\omega}{2\pi} f'_{\mathrm{N}}(\omega) g^{\mathrm{r}}(\boldsymbol{r},\omega) \times \tilde{t} A_{\mathrm{s},t} \tilde{t}^{\dagger} g^{\mathrm{a}}(-\boldsymbol{r},\omega). \tag{72}$$

(Diagrammatic representation of the contribution is in Fig. 8. For calculation detail, see Appendix C). For damping, off-diagonal contributions, $\mathcal{A}^{\pm}_{\mathrm{s},t}$, are obviously essential. The result of the spin density in F in the rotated frame, Eq. (68), is therefore

$$\begin{aligned}\tilde{s}^{(\mathrm{F})}_{\alpha}(\boldsymbol{r},t) &= 2\pi i \nu_{\mathrm{N}} a^2 \int \frac{d\omega}{2\pi} f'_{\mathrm{N}}(\omega) A^{\beta}_{\mathrm{s},t} \mathrm{tr}[\sigma_{\alpha} g^{\mathrm{r}}(\boldsymbol{r},\omega) \\ &\quad \times \tilde{t}\sigma_{\beta}\tilde{t}^{\dagger} g^{\mathrm{a}}(-\boldsymbol{r},\omega)] \\ &= 2\pi i \nu_{\mathrm{N}} a^2 \int \frac{d\omega}{2\pi} f'_{\mathrm{N}}(\omega) A^{\beta}_{\mathrm{s},t} \sum_{\boldsymbol{k}\boldsymbol{k}'} e^{i(\boldsymbol{k}-\boldsymbol{k}')\cdot\boldsymbol{r}} \\ &\quad \times \mathrm{tr}[\sigma_{\alpha} g^{\mathrm{r}}(\boldsymbol{k},\omega)\tilde{t}\sigma_{\beta}\tilde{t}^{\dagger} g^{\mathrm{a}}(\boldsymbol{k}',\omega)].\end{aligned} \tag{73}$$

Evaluating the trace in spin space, we obtain

$$\tilde{\boldsymbol{s}}^{(\mathrm{F})}(\boldsymbol{r},t) = -\nu_{\mathrm{N}}[\boldsymbol{A}^{\perp}_{\mathrm{s},t}\gamma_1(\boldsymbol{r}) + (\hat{\boldsymbol{z}} \times \boldsymbol{A}^{\perp}_{\mathrm{s},t})\gamma_2(\boldsymbol{r})], \tag{74}$$

where

$$\begin{aligned}\gamma_1(\boldsymbol{r}) &\equiv \sum_{\sigma} \tilde{t}_{-\sigma}\tilde{t}^{\dagger}_{\sigma} g^{\mathrm{r}}_{-\sigma}(\boldsymbol{r}) g^{\mathrm{a}}_{\sigma}(-\boldsymbol{r}), \\ \gamma_2(\boldsymbol{r}) &\equiv \sum_{\sigma} (-i\sigma)\tilde{t}_{-\sigma}\tilde{t}^{\dagger}_{\sigma} g^{\mathrm{r}}_{-\sigma}(\boldsymbol{r}) g^{\mathrm{a}}_{\sigma}(-\boldsymbol{r}).\end{aligned} \tag{75}$$

We consider an interface with infinite area and consider spin accumulation averaged over the plane parallel to the interface. The wave vectors contributing are then those with finite k_x but with $k_y = k_z = 0$ and the Green's function becomes one-dimensional-like:

$$\sum_{\boldsymbol{k}} e^{i\boldsymbol{k}\cdot\boldsymbol{r}} g^{\mathrm{r}}_{\sigma}(\boldsymbol{k}) = \frac{im}{k_{F\sigma}} e^{ik_{F\sigma}|x|} e^{-|x|/(2\ell_{\sigma})}, \tag{76}$$

where $\ell_{\sigma} \equiv v_{\mathrm{F}\sigma}\tau_{\sigma}$ ($v_{\mathrm{F}\sigma} \equiv k_{\mathrm{F}\sigma}/m$) is the electron mean free path for spin σ. The induced spin density in the ferromagnet is finally obtained from Eq. (74) as

$$\begin{aligned}\boldsymbol{s}^{(\mathrm{F})}(\boldsymbol{r},t) &= \frac{m^2\nu_{\mathrm{N}}a^2}{2k_{F+}k_{F-}} \sum_{\sigma} [(\boldsymbol{n}\times\dot{\boldsymbol{n}})\overline{T_{\sigma,-\sigma}} e^{-i\sigma(k_{F+}-k_{F-})x} \\ &\quad + \dot{\boldsymbol{n}}(-i\sigma)\overline{T_{\sigma,-\sigma}} e^{-i\sigma(k_{F+}-k_{F-})x}] \\ &= \frac{m^2\nu_{\mathrm{N}}a^2}{2k_{F+}k_{F-}} \sum_{\sigma} \{(\boldsymbol{n}\times\dot{\boldsymbol{n}})[\mathrm{Re}[\overline{T_{\uparrow,\downarrow}}]\cos((k_{F+}-k_{F-}) \\ &\quad \times x) + \mathrm{Im}[\overline{T_{\uparrow,\downarrow}}]\sin((k_{F+}-k_{F-})x)] \\ &\quad + \dot{\boldsymbol{n}}[\mathrm{Im}[\overline{T_{\uparrow,\downarrow}}]\cos((k_{F+}-k_{F-})x) \\ &\quad - \mathrm{Re}[\overline{T_{\uparrow,\downarrow}}]\sin((k_{F+}-k_{F-})x)]\}\end{aligned} \tag{77}$$

and the torque on the localized spin $-M\boldsymbol{n}\times\boldsymbol{s}^{(\mathrm{F})}$ is

$$\begin{aligned}\boldsymbol{\tau}(\boldsymbol{r},t) &= -\frac{m^2\nu_{\mathrm{N}}a^2 M}{2k_{F+}k_{F-}} \sum_{\sigma} \{-\dot{\boldsymbol{n}}[\mathrm{Re}[\overline{T_{\uparrow,\downarrow}}]\cos((k_{F+}-k_{F-})x) \\ &\quad + \mathrm{Im}[\overline{T_{\uparrow,\downarrow}}]\sin((k_{F+}-k_{F-})x)] \\ &\quad + (\boldsymbol{n}\times\dot{\boldsymbol{n}})[\mathrm{Im}[\overline{T_{\uparrow,\downarrow}}]\cos((k_{F+}-k_{F-})x) \\ &\quad - \mathrm{Re}[\overline{T_{\uparrow,\downarrow}}]\sin((k_{F+}-k_{F-})x)]\}.\end{aligned} \tag{78}$$

A. Enhanced damping and spin renormalization of ferromagnetic metal

The total induced spin accumulation density in a ferromagnet is

$$\begin{aligned}\overline{\boldsymbol{s}^{(\mathrm{F})}} &\equiv \frac{1}{d}\int_{-d}^{0} dx \boldsymbol{s}^{(\mathrm{F})}(x) \\ &= \frac{1}{M}\{(\boldsymbol{n}\times\dot{\boldsymbol{n}})[-\mathrm{Im}[\delta](1-\cos\tilde{d}) + \mathrm{Re}[\delta]\sin\tilde{d}] \\ &\quad + \dot{\boldsymbol{n}}[\mathrm{Re}[\delta](1-\cos\tilde{d}) + \mathrm{Im}[\delta]\sin\tilde{d}]\},\end{aligned} \tag{79}$$

where $\tilde{d} \equiv (k_{F+}-k_{F-})d$, d is the thickness of the ferromagnet and

$$\delta \equiv \frac{m^2\nu_{\mathrm{N}}a^2 M}{k_{F+}k_{F-}(k_{F+}-k_{F-})d}\overline{T_{\uparrow,\downarrow}}. \tag{80}$$

As a result of this induced electron spin density, $\overline{\boldsymbol{s}^{(\mathrm{F})}}$, the equation of motion for the averaged magnetization is modified to be [11]

$$\dot{\boldsymbol{n}} = -\alpha\boldsymbol{n}\times\dot{\boldsymbol{n}} - \gamma\boldsymbol{B}\times\boldsymbol{n} - M\boldsymbol{n}\times\overline{\boldsymbol{s}^{(\mathrm{F})}}, \tag{81}$$

where $\boldsymbol{B}$ is the external magnetic field.

Let us first discuss the thick ferromagnet case, $d \gg |k_{F+}-k_{F-}|^{-1}$, where the oscillating part with respect to $\tilde{d}$ is neglected. The spin density then reads $\overline{\boldsymbol{s}^{(\mathrm{F})}} \simeq \frac{1}{M}(-\mathrm{Im}[\delta](\boldsymbol{n}\times\dot{\boldsymbol{n}}) + \mathrm{Re}[\delta]\dot{\boldsymbol{n}})$ and the equation of motion becomes

$$(1+\mathrm{Im}\delta)\dot{\boldsymbol{n}} = -\tilde{\alpha}\boldsymbol{n}\times\dot{\boldsymbol{n}} - \gamma\boldsymbol{B}\times\boldsymbol{n}, \tag{82}$$

where

$$\tilde{\alpha} \equiv \alpha + \mathrm{Re}\delta, \tag{83}$$

is the Gilbert damping including the enhancement due to the spin pumping effect. The precession angular frequency ω_B is modified by the imaginary part of $T_{\uparrow,\downarrow}$, i.e., by the spin current

proportional to $\dot{\boldsymbol{n}}$, as

$$\omega_B = \frac{\gamma B}{1 + \mathrm{Im}\delta}. \tag{84}$$

This is equivalent to the modification of the gyromagnetic ratio (γ) or the g factor.

For most 3D ferromagnets, we may approximate $\frac{m^2 \nu_N a M {\epsilon_F}^2}{2k_{F+}k_{F-}(k_{F+}-k_{F-})} \simeq O(1)$ (as $k_{F+} - k_{F-} \propto M$), resulting in $\delta \sim \frac{a}{d} T_{\uparrow,\downarrow}$. As discussed in Sec. III, when the interface spin-orbit interaction is taken into account, we have $T_{\uparrow,\downarrow} = \tilde{t}^0_\uparrow \tilde{t}^0_\downarrow + i\tilde{\gamma}_{xz}(\tilde{t}^0_\uparrow + \tilde{t}^0_\downarrow) + O((\tilde{\gamma})^2)$, where $\tilde{t}^0_\sigma$ and $\tilde{\gamma}_{xz}$ are assumed to be real. Moreover, $\tilde{t}^0_\sigma$ can be chosen as positive and thus $T_{\uparrow,\downarrow} > 0$. ($\tilde{t}^0_\sigma$ here is field representation, and has unit of energy.) Equations (83) and (84) indicate that the strength of the hopping amplitude $\tilde{t}^0_\sigma$ and interface spin-orbit interaction $\tilde{\gamma}_{xz}$ are experimentally accessible by measuring the Gilbert damping and shift of resonance frequency as has been known [2]. A significant consequence of Eq. (83) is that the enhancement of the Gilbert damping,

$$\delta\alpha \sim \frac{a}{d}\frac{1}{{\epsilon_F}^2}\tilde{t}^0_\uparrow \tilde{t}^0_\downarrow, \tag{85}$$

can exceed in thin ferromagnets the intrinsic damping parameter α, as the two contributions are governed by different material parameters. In contrast to the positive enhancement of damping, the shift of the resonant frequency or g factor can be positive or negative, as it is linear in the interface spin-orbit parameter $\tilde{\gamma}_{xz}$.

Experimentally, the enhancement of the Gilbert damping and frequency shift has been measured in many systems [12]. In the case of $Ni_{80}Fe_{20}$(Py)/Pt junction, the enhancement of damping is observed to be proportional to $1/d$ in the range of $2\,\mathrm{nm} < d < 10\,\mathrm{nm}$, and the enhancement was large, $\delta\alpha/\alpha \simeq 4$ at $d = 2$ nm [12]. These results appears to be consistent with our analysis. Same $1/d$ dependence was observed in the shift of the g factor. The shift was positive and the magnitude is about 2% for Py/Pt and Py/Pd with $d = 2$nm, while it was negative for Ta/Pt [12]. The existence of both signs suggests that the shift is due to the linear effect of spin-orbit interaction, and the interface spin-orbit interaction we discuss is one of the possible mechanisms.

For thin ferromagnet, $\tilde{d} \lesssim 1$, the spin accumulation of Eq. (79) reads

$$\overline{\boldsymbol{s}^{(\mathrm{F})}} = \frac{1}{M}((\boldsymbol{n} \times \dot{\boldsymbol{n}})\mathrm{Re}[\delta_{\mathrm{thin}}] + \dot{\boldsymbol{n}}\mathrm{Im}[\delta_{\mathrm{thin}}]), \tag{86}$$

where

$$\delta_{\mathrm{thin}} \equiv \delta\tilde{d} = \frac{m^2 \nu_N a^2 M}{2k_{F+}k_{F-}}\overline{T_{\uparrow,\downarrow}}. \tag{87}$$

Equation (86) indicates that the roles of imaginary and real part of $\overline{T_{\uparrow,\downarrow}}$ are interchanged for thick and thin ferromagnets, resulting in

$$\tilde{\alpha} = \alpha + \mathrm{Im}\delta_{\mathrm{thin}}, \quad \omega_B = \frac{\gamma B}{1 - \mathrm{Re}\delta_{\mathrm{thin}}}, \tag{88}$$

for thin ferromagnets. Thus, for weak interface spin-orbit interaction, a positive shift of the resonance frequency is expected (as $\mathrm{Re}\delta_{\mathrm{thin}} > 0$). A significant feature is that the damping can be decreased or even become negative if strong interface spin-orbit interaction exists with a negative sign of $\mathrm{Im}\delta_{\mathrm{thin}}$. Our result indicates that the "spin mixing conductance" description of Ref. [2] breaks down in thin metallic ferromagnets (and the insulator case as we shall see in Sec. VII D).

In this section, we have discussed spin accumulation and enhanced Gilbert damping in a ferromagnet attached to a normal metal. In the field-theoretic description, the damping enhancement arises from the imaginary part of the self-energy due to the interface. Thus a randomness like the interface scattering changing the electron momentum is essential for the damping effect, which sounds physically reasonable. The same is true for the reaction, namely, the spin current pumping effect into the N region, and thus the spin current pumping requires randomness too. (In the quantum mechanical treatment of Sec. II, change of electron wave vector at the interface is essential.) The spin current pumping effect therefore appears different from general pumping effects, where randomness does not play essential roles apparently [3].

The spin accumulation and enhanced Gilbert damping was discussed by Berger [11] based on a quantum mechanical argument. There, $1/d$ dependence was pointed out and the damping effect was calculated by evaluating the decay rate of magnons. A comparison of enhanced Gilbert damping with experiments was carried out in Ref. [2] but in a phenomenological manner.

VI. CASE WITH MAGNETIZATION STRUCTURE

The field theoretic approach has an advantage that the generalization of the results is straightforward. Here we discuss briefly the case of a ferromagnet with spatially varying magnetization. The excitations in a metallic ferromagnet consist of spin waves (magnons) and Stoner excitation. While spin waves usually have a gap as a result of magnetic anisotropy, Stoner excitation is gapless for a finite wave vector, $(k_{F+} - k_{F-}) < |q| < (k_{F+} + k_{F-})$, and it may be expected to have significant contribution for magnetization structures having wavelength larger than $k_{F+} - k_{F-}$. Let us look into this possibility.

Our result of spin accumulation in a ferromagnet, represented in the rotated frame, Eq. (A3), indicates that when the magnetization has a spatial profile, the accumulation is determined by the spin gauge field and spin correlation function depending on the wave vector $\boldsymbol{q}$ as

$$\sum_{\boldsymbol{q}} \mathcal{A}^{\pm}_{\mathrm{s},t}(q)\chi_{\pm}(q,0), \tag{89}$$

where

$$\chi_{\pm}(\boldsymbol{q},\Omega) \equiv -\sum_{\boldsymbol{k}} \frac{f_{\boldsymbol{k}+\boldsymbol{q},\pm} - f_{\boldsymbol{k},\mp}}{\epsilon_{\boldsymbol{k}+\boldsymbol{q},\pm} - \epsilon_{\boldsymbol{k},\mp} + \Omega + i0} \tag{90}$$

is the correlation function with finite momentum transfer $\boldsymbol{q}$ and finite angular frequency Ω. For the case of free electron with quadratic dispersion, the correlation function is [34]

$$\chi_{\pm}(\boldsymbol{q},\Omega) = A_q + i\Omega B_q \theta_{\mathrm{st}}(q) + O(\Omega^2), \tag{91}$$

where

$$A_q = \frac{ma^3}{8\pi^2}\Bigg[(k_{F+}+k_{F-})\left(1+\frac{(k_{F+}-k_{F-})^2}{q^2}\right) + \frac{1}{2q^3}((k_{F+}+k_{F-})^2-q^2)(q^2-(k_{F+}-k_{F-})^2) \times \ln\left|\frac{q+(k_{F+}+k_{F-})}{q-(k_{F+}+k_{F-})}\right|\Bigg],$$
$$B_q = \frac{m^2a^3}{4\pi|q|}, \tag{92}$$

and

$$\theta_{\rm st}(q) \equiv \begin{cases} 1 & (k_{F+}-k_{F-}) < |q| < (k_{F+}+k_{F-}) \\ 0 & \text{otherwise} \end{cases}, \tag{93}$$

describes the wave vectors where Stoner excitation exists. As we see from Eq. (91), the Stoner excitation contribution vanishes to the lowest order in Ω, and thus the spin pumping effect in the adiabatic limit ($\Omega \to 0$) is not affected. Moreover, the real part of the correlation function, A_q, is a decreasing function of q and thus the spin pumping efficiency would decrease when the ferromagnet has a structure. However, for rigorous argument, we need to include the spatial component of the spin gauge field arising form the spatial derivative of the magnetization profile.

As for the effect of the Stoner excitation on spin damping (Gilbert damping), it was demonstrated for the case of a domain wall that the effect is negligibly small for a wide wall with thickness $\lambda \gg (k_{F+}-k_{F-})^{-1}$ (Refs. [34,35]). Simanek and Heinrich presented a result of the Gilbert damping as the linear term in the frequency of the imaginary part of the spin correlation function integrated over the wave vector [13]. The result is, however, obtained for a model where the ferromagnet is an atomically thin layer (a sheet), and would not be applicable for most experimental situations. A discussion of the Gilbert damping including a finite wave vector and the impurity scattering was given in Ref. [36]. Inhomogeneity effects of damping of a domain wall were studied recently in detail [37]. The effective Gilbert damping constant in the presence of a domain wall was numerically studied in Refs. [38,39]. A quadratic dependence on the inverse of the wall thickness appears to be consistent with the quadratic behavior of A_q at small q, while the linear behavior found for an out-of-plane extremely narrow wall [39] seems not to be covered by the simple argument here.

VII. INSULATOR FERROMAGNET

In this section, we discuss the case of a ferromagnetic insulator. It turns out that the generation mechanisms for spin current in the insulating and metallic cases are distinct.

A. Magnon and adiabatic gauge field

The Lagrangian for the insulating ferromagnet is

$$L_{\rm IF} = \int d^3r\left[S\dot{\phi}(\cos\theta-1) - \frac{J}{2}(\nabla \boldsymbol{S})^2\right] - H_K, \tag{94}$$

where J is the exchange interaction between the localized spin $\boldsymbol{S}$ and H_K denotes the magnetic anisotropy energy.

We first study low-energy magnon dynamics induced by slow magnetization dynamics. For separating the classical variable and fluctuation (magnon), the rotated coordinate description used in the metallic case is convenient. For magnons described by the Holstein-Primakov boson, the unitary transformation is a 3×3 matrix defined as follows [40]:

$$\boldsymbol{S} = U\widetilde{\boldsymbol{S}}, \tag{95}$$

where

$$U = \begin{pmatrix} \cos\theta\cos\phi & -\sin\phi & \sin\theta\cos\phi \\ \cos\theta\sin\phi & \cos\phi & \sin\theta\sin\phi \\ -\sin\theta & 0 & \cos\theta \end{pmatrix} = \begin{pmatrix} \boldsymbol{e}_\theta & \boldsymbol{e}_\phi & \boldsymbol{n} \end{pmatrix}. \tag{96}$$

The diagonalized spin $\widetilde{\boldsymbol{S}}$ is represented in terms of annihilation and creation operators for the Holstein-Primakov boson, b and $b^\dagger$, as [41]

$$\widetilde{\boldsymbol{S}} = \begin{pmatrix} \sqrt{\frac{S}{2}}(b^\dagger+b) \\ i\sqrt{\frac{S}{2}}(b^\dagger-b) \\ S-b^\dagger b \end{pmatrix}. \tag{97}$$

We neglect the terms that are third- and higher-order in boson operators. Derivatives of the localized spin then read

$$\partial_\mu \boldsymbol{S} = U(\partial_\mu + iA_{U,\mu})\widetilde{\boldsymbol{S}}, \tag{98}$$

where

$$A_{U,\mu} \equiv -iU^{-1}\nabla_\mu U \tag{99}$$

is the spin gauge field represented as a 3×3 matrix. The spin Berry's phase of the Lagrangian (94) is written in terms of magnons as (derivation is in Appendix D)

$$L_{\rm m} = 2S\gamma^2\int d^3r i\left[b^\dagger\left(\partial_t + i\mathcal{A}^z_{{\rm s},t}\right)b - b^\dagger\left(\overleftarrow{\partial}_t - i\mathcal{A}^z_{{\rm s},t}\right)b\right], \tag{100}$$

namely, the magnons interact with the adiabatic component of the same spin gauge field for electrons, $\mathcal{A}^z_{{\rm s},t}$, defined in Eq. (14). As the magnon is a single-component field, the gauge field is also single-component, i.e., a U(1) gauge field. This is a significant difference between insulating and metallic ferromagnets; in the metallic case, a conduction electron couples to an SU(2) gauge field with spin-flip components, which turned out to be essential for spin current generation. In contrast, in the insulating case, the magnon has a diagonal gauge field, i.e., a spin chemical potential, which simply induces diagonal spin polarization. Pumping of magnon was discussed in a different approach by evaluating the magnon source term in Ref. [42].

The exchange interaction at the interface is represented by a Hamiltonian

$$H_{\rm I} = J_{\rm I}\int d^3r_{\rm I}\boldsymbol{S}(\boldsymbol{r})\cdot c^\dagger\boldsymbol{\sigma}c, \tag{101}$$

where $J_{\rm I}$ is the strength of the interface sd exchange interaction and the integral is over the interface. We consider a sharp interface at $x=0$. Using Eq. (95), the interaction is represented

in terms of magnon operators up to the second order as

$$H_{\rm I} = J_{\rm I}\int d^3r_{\rm I}\Big\{(S-b^\dagger b)c^\dagger(\boldsymbol{n}\cdot\boldsymbol{\sigma})c + \sqrt{\frac{S}{2}}[b^\dagger c^\dagger\boldsymbol{\Phi}\cdot\boldsymbol{\sigma}c + bc^\dagger\boldsymbol{\Phi}^*\cdot\boldsymbol{\sigma}c]\Big\}, \quad (102)$$

where

$$\boldsymbol{\Phi}\equiv\boldsymbol{e}_\theta + i\boldsymbol{e}_\phi = \begin{pmatrix}\cos\theta\cos\phi - i\sin\phi\\ \cos\theta\sin\phi + i\cos\phi\\ -\sin\theta\end{pmatrix}. \quad (103)$$

Equation (102) indicates that there are two mechanisms for spin current generation; namely, the one due to the magnetization at the interface (the term proportional to $\boldsymbol{n}$) and the one due to the magnon spin scattering at the interface (described by the term linear in magnon operators).

Let us briefly demonstrate based on the expression of Eq. (102) that spin-flip processes due to magnon creation or annihilation lead to generation of spin current in the normal metal. At the second order, the interaction induces a factor on the electron wave function $(\boldsymbol{\Phi}^*(t)\cdot\boldsymbol{\sigma})(\boldsymbol{\Phi}(t')\cdot\boldsymbol{\sigma})$ for magnon creation and $(\boldsymbol{\Phi}(t)\cdot\boldsymbol{\sigma})(\boldsymbol{\Phi}^*(t')\cdot\boldsymbol{\sigma})$ for annihilation (we allow an infinitesimal difference in time t and t'). The factor for the creation has charge and spin contributions, $(\boldsymbol{\Phi}^*(t)\cdot\boldsymbol{\sigma})(\boldsymbol{\Phi}(t')\cdot\boldsymbol{\sigma}) = \boldsymbol{\Phi}^*(t)\cdot\boldsymbol{\Phi}(t') + i\boldsymbol{\sigma}\cdot(\boldsymbol{\Phi}^*(t)\times\boldsymbol{\Phi}(t'))$. For magnon annihilation, we have $(\boldsymbol{\Phi}^*(t)\times\boldsymbol{\Phi}(t'))^*$, and thus the sum of the magnon creation and annihilation processes leads to a factor

$$\sum_{\boldsymbol{q}}[(n_{\boldsymbol{q}}+1)(\boldsymbol{\Phi}^*(t)\times\boldsymbol{\Phi}(t')) + n_{\boldsymbol{q}}(\boldsymbol{\Phi}^*(t)\times\boldsymbol{\Phi}(t'))^*] = \sum_{\boldsymbol{q}}\{(2n_{\boldsymbol{q}}+1){\rm Re}[\boldsymbol{\Phi}^*(t)\times\boldsymbol{\Phi}(t')] + i{\rm Im}[\boldsymbol{\Phi}^*(t)\times\boldsymbol{\Phi}(t')]\}. \quad (104)$$

For adiabatic change, the amplitude is expanded as

$$(\boldsymbol{\Phi}^*(t)\times\boldsymbol{\Phi}(t')) = 2i(1+i(t-t')\cos\theta\dot\phi)\boldsymbol{n} - (t-t')\times(\boldsymbol{n}\times\dot{\boldsymbol{n}} - i\ddot{\boldsymbol{n}}) + O((\partial_t)^2), \quad (105)$$

where we see that a retardation effect from the adiabatic change of magnetization (represented by the second term on the right-hand side) gives rise to a magnon state change proportional to $\boldsymbol{n}\times\dot{\boldsymbol{n}}$ and $\ddot{\boldsymbol{n}}$. The retardation contribution for the spin part [Eq. (104)] is

$$(t-t')\sum_{\boldsymbol{q}}[-(2n_{\boldsymbol{q}}+1)(\boldsymbol{n}\times\dot{\boldsymbol{n}}) + i\ddot{\boldsymbol{n}}]. \quad (106)$$

We therefore expect that a spin current proportional to $\boldsymbol{n}\times\dot{\boldsymbol{n}}$ emerges proportional to the magnon creation and annihilation number, $\sum_{\boldsymbol{q}}(2n_{\boldsymbol{q}}+1)$. (As we shall see below, the factor $t-t'$ reduces to a derivative with respect to the angular frequency of the Green's function.) A rigorous estimation using the Green's function method is presented in Sec. VII C.

In Eq. (106), the last term proportional to $\ddot{\boldsymbol{n}}$ is an imaginary part arising from the difference of magnon creation and annihilation probabilities of vacuum, $n_{\boldsymbol{q}}+1$ and $n_{\boldsymbol{q}}$. The term is, however, an unphysical one corresponding to a real energy shift due to magnon interaction, and is removed by redefinition of the Fermi energy.

FIG. 9. Feynman diagrams for spin current pumped by interface sd exchange interaction.

B. Spin current pumped by the interface exchange interaction

Here, we study the spin current pumped by the classical magnetization at the interface, namely, the one driven by the term proportional to $S\boldsymbol{n}$ in Eq. (102). We treat the exchange interaction perturbatively to the second order as the exchange interaction between a conduction electron and the insulator ferromagnet is localized at the interface and is expected to be weak. The weak-coupling scheme employed here is in the opposite limit as the strong-coupling (adiabatic) approach used in the metallic ferromagnet (Sec. IV). A recent experiment indicates that the insulator spin pumping effect is driven by local magnetization induced in the normal metal by the magnetic proximity effect [8], supporting perturbative treatment.

In the perturbative regime, the issue of adiabaticity needs to be argued carefully. In the strong sd coupling limit, the adiabaticity is trivially satisfied, as the time needed for the electron spin to follow the localized spin is the fastest time scale. In the weak-coupling limit, this time scale is long. Nevertheless, the adiabatic condition is satisfied if the electron spin relaxation is strong so that the electron spin relaxes quickly to the local equilibrium state determined by the localized spin. Thus the adiabatic condition is expected to be $M_{\rm I}\tau_{\rm sf}/\hbar \ll 1$, where $M_{\rm I}$ and $\tau_{\rm sf}$ are the interface spin splitting energy, and the conduction electron spin relaxation time, respectively. In the following calculation, we consider the case of $\epsilon_F\tau_{\rm sf}/\hbar \gg 1$, i.e., $\hbar(\tau_{\rm sf})^{-1} \ll \epsilon_F$, as the spin-flip lifetime is by definition longer than the elastic electron lifetime τ, which satisfies $\epsilon_F\tau/\hbar \gg 1$ in a metal. The perturbative results therefore can apply to both adiabatic and nonadiabatic cases.

The calculation is carried out by evaluating the Feynman diagrams of Fig. 9, similar to the study of Refs. [18,19]. A difference is that while Refs. [18,19] assumed a smooth magnetization structure and used a gradient expansion, the exchange interaction we consider is localized.

The lesser Green's function for a normal metal including the interface exchange interaction to the linear order is

$$G^{(1)<}_{\rm N}(\boldsymbol{r},t,\boldsymbol{r},t) = M_{\rm I}\int\frac{d\omega}{2\pi}\int\frac{d\Omega}{2\pi}\sum_{\boldsymbol{k}\boldsymbol{k}'}e^{-i\Omega t}e^{i(\boldsymbol{k}'-\boldsymbol{k})\cdot\boldsymbol{r}} \times\Big[(f(\omega+\Omega)-f(\omega))g^{\rm r}_{\boldsymbol{k}',\omega+\Omega}g^{\rm a}_{\boldsymbol{k}\omega} - f(\omega)g^{\rm r}_{\boldsymbol{k}',\omega+\Omega}g^{\rm r}_{\boldsymbol{k}\omega} + f(\omega+\Omega)g^{\rm a}_{\boldsymbol{k}',\omega+\Omega}g^{\rm a}_{\boldsymbol{k}\omega}\Big] \times(\boldsymbol{n}_\Omega\cdot\boldsymbol{\sigma}), \quad (107)$$

where $M_{\rm I}\equiv J_{\rm I}S$ is the local spin polarization at the interface. Expanding the expression with respect to Ω and keeping the dominant contribution at long distance, i.e., the terms containing both $g^{\rm a}$ and $g^{\rm r}$. Using $\sum_{\boldsymbol{k}}g^{\rm a}_{\boldsymbol{k}\omega}e^{i\boldsymbol{k}\cdot\boldsymbol{r}} \simeq \frac{im}{k_F}e^{ikr}e^{-\frac{|x|}{\ell}}(\equiv$

$g^{\rm a}(\boldsymbol{r})$), the result of spin current is

$$j_{\rm s}^{(1)}(\boldsymbol{r},t) = -M_{\rm I}\frac{m}{k_F}\dot{\boldsymbol{n}}e^{-|x|/\ell}. \tag{108}$$

The second-order contribution is similarly calculated to obtain

$$\begin{aligned} G_{\rm N}^{(2)<}(\boldsymbol{r},t,\boldsymbol{r},t) \simeq (M_{\rm I})^2 \int\frac{d\omega}{2\pi}\int\frac{d\Omega_1}{2\pi}\int\frac{d\Omega_2}{2\pi} \\ \times \sum_{\boldsymbol{k}\boldsymbol{k}'\boldsymbol{k}''} e^{-i(\Omega_1+\Omega_2)t}e^{i(\boldsymbol{k}'-\boldsymbol{k})\cdot\boldsymbol{r}} f'(\omega) g^{\rm r}_{\boldsymbol{k}',\omega} g^{\rm a}_{\boldsymbol{k}\omega} \\ \times \left(\Omega_1 g^{\rm a}_{\boldsymbol{k}''\omega} + \Omega_2 g^{\rm r}_{\boldsymbol{k}''\omega}\right)\left(\boldsymbol{n}_{\Omega_1}\cdot\boldsymbol{\sigma}\right)\left(\boldsymbol{n}_{\Omega_2}\cdot\boldsymbol{\sigma}\right) \\ = -2\pi i \nu (M_{\rm I})^2 |g^{\rm r}(\boldsymbol{r})|^2 (\boldsymbol{n}\times\dot{\boldsymbol{n}})\cdot\boldsymbol{\sigma}. \end{aligned} \tag{109}$$

The corresponding spin current at the interface ($x = 0$) is thus

$$j_{\rm s}^{(2)}(x=0,t) = \nu (M_{\rm I})^2 \frac{m}{k_F}(\boldsymbol{n}\times\dot{\boldsymbol{n}}), \tag{110}$$

and the total spin current reads

$$j_{\rm s}(x=0,t) = -M_{\rm I}\frac{m}{k_F}\dot{\boldsymbol{n}} - 2\nu (M_{\rm I})^2 \frac{m}{k_F}(\boldsymbol{n}\times\dot{\boldsymbol{n}}). \tag{111}$$

In the perturbation regime, the spin current proportional to $\dot{\boldsymbol{n}}$ is dominant (larger by a factor of $(\nu M_{\rm I})^{-1}$) compared to the one proportional to $\boldsymbol{n}\times\dot{\boldsymbol{n}}$.

An expression of the spin current induced by the interface exchange interaction was presented in Ref. [43] in the limit of strong spin relaxation, $M_{\rm I}\tau_{\rm sf} \ll 1$, where $\tau_{\rm sf}$ is the spin relaxation time of electrons. By solving the Landau-Lifshitz-Gilbert equation for the electron spin, they obtained Eq. (111) with $\nu M_{\rm I}$ replaced by $M_{\rm I}\tau_{\rm sf}$.

C. Calculation of magnon-induced spin current

Here, the magnon-induced spin current due to the magnon interaction in Eq. (102) is calculated. As a magnon is a small fluctuation of magnetization, the contribution here is a small correction to the contribution of Eq. (111). Nevertheless, the magnon contribution has a typical linear dependence on the temperature, and is expected to be experimentally identified easily.

The spin current induced in a normal metal is evaluated by calculating the self-energy arising from the interface magnon scattering of Eq. (102). The contribution to the path-ordered Green's function of N electron from the magnon scattering to the second order is

$$\begin{aligned} G_{\rm N}(\boldsymbol{r},t,\boldsymbol{r}'.t') = \int_C dt_1 \int_C dt_2 \sum_{\boldsymbol{r}_1\boldsymbol{r}_2} g_{\rm N}(\boldsymbol{r},t,\boldsymbol{r}_1,t_1) \\ \times \Sigma_{\rm I}(\boldsymbol{r}_1,t_1,\boldsymbol{r}_2,t_2) g_{\rm N}(\boldsymbol{r}_2,t_2,\boldsymbol{r}',t'), \end{aligned} \tag{112}$$

where

$$\Sigma_{\rm I}(\boldsymbol{r}_1,t_1,\boldsymbol{r}_2,t_2) \equiv i\frac{SJ_{\rm I}^2}{2}\mathcal{D}_{\alpha\beta}(\boldsymbol{r}_1,t_1,\boldsymbol{r}_2,t_2)\sigma_\alpha g_{\rm N}(\boldsymbol{r}_1,t_1,\boldsymbol{r}_2,t_2)\sigma_\beta \tag{113}$$

represents the self-energy. Here,

$$\mathcal{D}_{\alpha\beta}(\boldsymbol{r}_1,t_1,\boldsymbol{r}_2,t_2) \equiv -i\langle T_C \mathcal{B}_\alpha(\boldsymbol{r}_1,t_1)\mathcal{B}_\beta(\boldsymbol{r}_2,t_2)\rangle \tag{114}$$

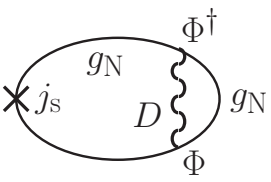

FIG. 10. Feynman diagrams for spin current pumped by magnons at the interface. Green's functions for magnons and electrons in the normal metal are denoted by D and $g_{\rm N}$, respectively. Φ represents the effects of magnetization dynamics [Eq. (103)].

is the Green's function for a magnon dressed by the magnetization structure [$\boldsymbol{\Phi}$ is defined in Eq. (103)],

$$\mathcal{B}_\alpha(\boldsymbol{r},t) \equiv \Phi_\alpha(t) b^\dagger(\boldsymbol{r},t) + \Phi_\alpha^\dagger(t) b(\boldsymbol{r},t). \tag{115}$$

The diagrammatic representation is in Fig. 10. In the present approximation including the interface scattering to the second order, the electron Green's function in Eq. (113) is treated as spin-independent, resulting in a self-energy (defined on complex time contour)

$$\begin{aligned} \Sigma_{\rm I}(\boldsymbol{r}_1,t_1,\boldsymbol{r}_2,t_2) = i\frac{SJ_{\rm I}^2}{2}(\delta_{\alpha\beta} + i\epsilon_{\alpha\beta\gamma}\sigma_\gamma) \\ \times \mathcal{D}_{\alpha\beta}(\boldsymbol{r}_1,t_1,\boldsymbol{r}_2,t_2) g_{\rm N}(\boldsymbol{r}_1,t_1,\boldsymbol{r}_2,t_2). \end{aligned} \tag{116}$$

We focus on the spin-polarized contribution containing the Pauli matrix. The self-energy is then

$$\Sigma_{{\rm I},\gamma}(\boldsymbol{r}_1,t_1,\boldsymbol{r}_2,t_2) \equiv -\frac{SJ_{\rm I}^2}{2}\widetilde{\mathcal{D}}_\gamma(\boldsymbol{r}_1,t_1,\boldsymbol{r}_2,t_2) g_{\rm N}(\boldsymbol{r}_1,t_1,\boldsymbol{r}_2,t_2), \tag{117}$$

where $\widetilde{\mathcal{D}}_\gamma \equiv \epsilon_{\alpha\beta\gamma}\mathcal{D}_{\alpha\beta}$, and the lesser Green's function, Eq. (112), reads

$$G_{\rm N}^< = \sigma_\gamma G_{{\rm N},\gamma}^<, \tag{118}$$

where (time and spatial coordinates partially suppressed)

$$\begin{aligned} G_{{\rm N},\gamma}^<(\boldsymbol{r},t,\boldsymbol{r}'.t') \equiv \int_{-\infty}^{\infty} dt_1 \int_{-\infty}^{\infty} dt_2 \big[g_{\rm N}^{\rm r}(t-t_1)\Sigma_{{\rm I},\gamma}^{\rm r}(t_1,t_2) \\ \times g_{\rm N}^<(t_2-t') + g_{\rm N}^{\rm r}\Sigma_{{\rm I},\gamma}^< g_{\rm N}^{\rm a} + g_{\rm N}^<\Sigma_{{\rm I},\gamma}^{\rm a} g_{\rm N}^{\rm a}\big]. \end{aligned} \tag{119}$$

The dominant contribution long distance is (see Appendix E for detail)

$$G_{{\rm N},\gamma}^<(\boldsymbol{r},t,\boldsymbol{r}',t) \simeq \int\frac{d\omega}{2\pi}\sum_{\boldsymbol{k}\boldsymbol{k}'} g^{\rm r}_{{\rm N},\boldsymbol{k}\omega} g^{\rm a}_{{\rm N},\boldsymbol{k}'\omega} e^{i\boldsymbol{k}\cdot\boldsymbol{r}} e^{-i\boldsymbol{k}'\cdot\boldsymbol{r}'} \widetilde{\Sigma}_{{\rm I},\gamma} \tag{120}$$

with

$$\widetilde{\Sigma}_{{\rm I},\gamma} \simeq i\Psi_\gamma \frac{\pi\nu}{\epsilon_F}\frac{SJ_{\rm I}^2}{2}\sum_{\boldsymbol{q}\boldsymbol{k}''}(1+2n_{\boldsymbol{q}})(2f_{\boldsymbol{k}''} - f_{\boldsymbol{k}} - f_{\boldsymbol{k}'}). \tag{121}$$

The spin current pumped by the magnon scattering is therefore

$$\boldsymbol{j}_{\rm s}^{\rm m}(\boldsymbol{r},t) = \frac{\pi\nu}{\epsilon_F}\frac{SJ_{\rm I}^2}{2}|g^{\rm r}(\boldsymbol{r})|^2\sum_{\boldsymbol{q}}(1+2n_{\boldsymbol{q}})(\boldsymbol{n}\times\dot{\boldsymbol{n}}). \tag{122}$$

At high temperature compared to magnon energy, $\beta\omega_q \ll 1$, $1+2n_{\boldsymbol{q}} \simeq \frac{2k_BT}{\omega_{\boldsymbol{q}}}$, and the magnon-induced spin current depends linearly on temperature. The result (122) agrees with a previous study carried out in the context of thermally induced spin current [20].

D. Correction to Gilbert damping in the insulating case

In this section, we calculate the correction to the Gilbert damping and g factor of an insulating ferromagnet as a result of the spin pumping effect. We study the torque on the ferromagnetic magnetization arising from the effect of conduction electrons of a normal metal, given by

$$\boldsymbol{\tau}_{\rm I} = \boldsymbol{B}_{\rm I} \times \boldsymbol{n} = M_{\rm I}(\boldsymbol{n} \times \boldsymbol{s}_{\rm I}), \tag{123}$$

where

$$\boldsymbol{B}_{\rm I} \equiv -\frac{\delta H_{\rm I}}{\delta \boldsymbol{n}} = -M_{\rm I}\boldsymbol{s}_{\rm I} \tag{124}$$

is the effective magnetic field arising from the interface electron spin polarization, $\boldsymbol{s}_{\rm I}(t) \equiv -i{\rm tr}[\boldsymbol{\sigma} G^<_{\rm N}(0,t)]$. The contribution to the electron spin density linear in the interface exchange interaction, Eq. (101), is

$$s_{\rm I}^{(1),\alpha}(t) = -i\int dt_1 M_{\rm I} n_\beta(t_1){\rm tr}[\sigma_\alpha g_{\rm N}(t,t_1)\sigma_\beta g_{\rm N}(t_1,t)]^<, \tag{125}$$

where the Green's functions connect positions at the interface, i.e., from $x=0$ to $x=0$, and are spin unpolarized. (The Feynman diagrams for the spin density are the same as the one for the spin current, Fig. 9, with the vertex $j_{\rm s}$ replaced by the Pauli matrix.) The pumped contribution proportional to the time variation of magnetization is obtained as

$$\begin{aligned}\boldsymbol{s}_{\rm I}^{(1)}(t) &= -M_{\rm I}\dot{\boldsymbol{n}}\int\frac{d\omega}{2\pi}\sum_{\boldsymbol{k}\boldsymbol{k}'} f'(\omega)\left(g^{\rm a}_{{\rm N},\boldsymbol{k}'} - g^{\rm r}_{{\rm N},\boldsymbol{k}'}\right)\left(g^{\rm a}_{{\rm N},\boldsymbol{k}} - g^{\rm r}_{{\rm N},\boldsymbol{k}}\right)\\ &= -M_{\rm I}(\pi\nu)^2\dot{\boldsymbol{n}}.\end{aligned} \tag{126}$$

The second-order contribution similarly reads

$$\begin{aligned}s_{\rm I}^{(2),\alpha}(t) &= -\frac{i}{2}\int dt_1\int dt_2 (M_{\rm I})^2 n_\beta(t_1) n_\gamma(t_2){\rm tr}[\sigma_\alpha g_{\rm N}(t,t_1)\\ &\quad\times\sigma_\beta g_{\rm N}(t_1,t_2)\sigma_\gamma g_{\rm N}(t_2,t)]^<\\ &\simeq -2(M_{\rm I})^2(\pi\nu)^3(\boldsymbol{n}\times\dot{\boldsymbol{n}}).\end{aligned} \tag{127}$$

The interface torque is therefore

$$\boldsymbol{\tau}_{\rm I} = -(M_{\rm I}\pi\nu)^2(\boldsymbol{n}\times\dot{\boldsymbol{n}}) + 2(M_{\rm I}\pi\nu)^3\dot{\boldsymbol{n}}. \tag{128}$$

Including this torque in the LLG equation, $\dot{\boldsymbol{n}} = -\alpha\boldsymbol{n}\times\dot{\boldsymbol{n}} - \gamma\boldsymbol{B}\times\boldsymbol{n} + \boldsymbol{\tau}$, we have

$$(1-\delta_{\rm I})\dot{\boldsymbol{n}} = -\alpha_{\rm I}(\boldsymbol{n}\times\dot{\boldsymbol{n}}) - \gamma\boldsymbol{B}\times\boldsymbol{n}, \tag{129}$$

where

$$\delta_{\rm I} = 2\mu_d(\pi M_{\rm I}\nu)^3, \quad \alpha_{\rm I} = \alpha + \mu_d(\pi M_{\rm I}\nu)^2, \tag{130}$$

where $\mu_d \sim d_{\rm mp}/d$ is the ratio of the length of magnetic proximity ($d_{\rm mp}$) and thickness of the ferromagnet, d. The Gilbert damping constant therefore increases as far as the interface spin-orbit interaction is neglected. The resonance frequency is $\omega_B = \frac{\gamma B}{1-\delta_{\rm I}}$, and the shift can have both signs depending on the sign of interface exchange interaction, $M_{\rm I}$.

There may be a possibility that magnon excitations induce a torque that corresponds to effective damping. In fact, such a torque arises if $\langle b\rangle$ or $\langle b^\dagger\rangle$ are finite, i.e., if the magnon Bose condensation glows. Such condensation can in principle develop from the interface interaction of magnon creation or annihilation induced by electron spin flip, Eq. (102). However, conventional spin relaxation processes arising from the second order of random spin scattering do not contribute to such magnon condensation and additional damping.

Comparing the result of pumped spin current, Eq. (111), and that of damping coefficient, Eq. (130), we notice that the "spin mixing conductance" argument [2], where the coefficients for the spin current component proportional to $\boldsymbol{n}\times\dot{\boldsymbol{n}}$ and the enhancement of the Gilbert damping constant are governed by the same quantity (the real part of a spin mixing conductance) does not hold for the insulator case. In fact, our result indicates that the spin current component proportional to $\boldsymbol{n}\times\dot{\boldsymbol{n}}$ arises from the second-order correction to the interaction (the second diagram of Fig. 9), while the damping correction arises from the first-order process (the first diagram of Fig. 9). Although the magnitudes of the two effects happen to be both second order of the interface spin splitting, $M_{\rm I}$, the physical origins appear to be distinct. From our analysis, we see that the spin mixing conductance description is not general and applies only to the case of a thick metallic ferromagnet (see Sec. V A for the metallic case).

VIII. DISCUSSION

Our results are summarized in Table II. Let us discuss experimental results in the light of our results. In the early ferromagnetic resonance (FMR) experiments, consistent studies of g factor and the Gilbert damping were carried out on metallic ferromagnets [12]. The results appear to be consistent with theories (Refs. [2,11] and the present paper). Both the damping constant and the g factor have $1/d$ dependence on the thickness of the ferromagnet in the range of 2 nm $< d <$ 10 nm [12]. The maximum additional damping reaches $\delta\alpha \sim 0.1$ at $d = 2$ nm, which exceeds the original value of $\alpha \sim 0.01$. The g-factor modulation is about 1% at $d = 2$ nm, and its sign depends on the material; the g factor increases for Pd/Py/Pd and Pt/Py/Pt, while decreases for Ta/Py/Ta. These results appear consistent with ours, because $\delta\omega_B$ is governed by ${\rm Im}\overline{T_{+-}}$, whose sign depends on the sign of interface spin-orbit interaction. In contrast, damping enhancement proportional to ${\rm Re}\overline{T_{+-}}$ is positive for thick metals. However, other possibilities like the effect of a large interface orbital moment playing a role in the g factor, cannot be ruled out at present.

Recently, inverse spin Hall measurement has become common for detecting the spin current. In this method, however, only the dc component proportional to $\boldsymbol{n}\times\dot{\boldsymbol{n}}$ is accessible so far and there remains an ambiguity for qualitative estimates because another phenomenological parameter, the conversion efficiency from spin to charge, enters. Qualitatively, the values of $A_{\rm r}$ obtained by the inverse spin Hall measurements [44] and FMR measurements are consistent with each other.

The cases of insulating ferromagnets have been studied recently. In the early experiments, orders of magnitude smaller values of $A_{\rm r}$ compared to metallic cases were reported [43], while those small values are now understood as due to poor interface quality. In fact, FMR measurements on epitaxially grown samples like yttrium iron garnet

TABLE II. Summary of essential parameters determining the spin current j_s, corrections to the Gilbert damping $\delta\alpha$, and the resonance frequency shift $\delta\omega_B$ for metallic and insulating ferromagnets. Coefficients A_i and A_r are for the spin current, defined by Eq. (1). Label "–" indicates that it is not discussed in the present paper. "*" is for the strong spin relaxation case, the density of states ν is replaced by the inverse of electron spin-flip time τ_{sf} [43].

Ferromagnet (F)	A_i	A_r	$\delta\alpha$	$\delta\omega_B$	Assumption	Equations
			$\mathrm{Re}\overline{T_{+-}}$	$\mathrm{Im}\overline{T_{+-}}$	Thick F	(27)(63) (83)(84)
Metal	$\mathrm{Im}\overline{T_{+-}}$	$\mathrm{Re}\overline{T_{+-}}$				
			$\mathrm{Im}\overline{T_{+-}}$	$\mathrm{Re}\overline{T_{+-}}$	Thin F	(88)
Insulator	$M_I\nu$	$(M_I\nu)^2$	$(M_I\nu)^2$	$(M_I\nu)^3$	Weak spin relaxation*	(111) (130)
	–	$(M_I\nu)^2\sum_{\boldsymbol{q}}(1+2n_{\boldsymbol{q}})$	–	–	Magnon	(122)

($Y_3Fe_5O_{12}$,YIG)/Au/Fe turned out to show A_r of 1–5 $\times$ 10^{18} m^{-2} (Refs. [45,46]), which is the same order as in the metallic cases. Inverse spin Hall measurements on YIG/Pt report similar values [47], and the value is consistent with the first-principles calculation [48]. Systematic studies of YIG/NM with NM=Pt, Ta, W, Au, Ag, Cu, Ti, V, Cr, Mn, etc., were carried out with the result of $A_r \sim 10^{17}$–10^{18} m^{-2} (Refs. [49–52]). If we use a naive phenomenological relation, Eq. (6), $A_r = 10^{18}$ m^{-2} corresponds to $\delta\alpha = 3\times10^{-4}$ if $a = 2$ Å, $S = 1$, and $d = 20$ Å. Assuming interface sd exchange interaction, the value indicates $M_I\nu \sim 0.01$, which appears reasonable at least by the order of magnitude from the result of x-ray magnetic circular dichroism (XMCD) suggesting spin polarization of interface Pt of $0.05\mu_B$ within a proximity length of less than 1 nm [53]. A recent experiment indicates that the spin pumping effect of an insulator is induced locally in the normal metal as a result of the magnetic proximity effect [8], supporting our perturbative treatment.

On the other hand, FMR frequency shift of insulators cannot be explained by our theory. In fact, the shift for YIG/Pt is $\delta\omega_B/\omega_B \sim 1.6\times10^{-2}$, which is larger than $\delta\alpha \sim 2\times10^{-3}$, while our perturbation theory assuming weak interface sd interaction predicts $\delta\omega_B/\omega_B < \delta\alpha$. We expect that the discrepancy arises from the interface spin-orbit interaction that would be present at the insulator-metal interface, which modifies the magnetic proximity effect and damping torque significantly. It would be necessary to introduce an anomalous sd coupling at the interface like the one discussed in Ref. [54]. Experimentally, the influence of interface spin-orbit interaction [55] and proximity effect needs to be carefully characterized by using a microscopic technique such as MCD to compare with theories.

IX. SUMMARY

We have presented a microscopic study of spin pumping effects, the generation of spin current in a ferromagnet-normal metal junction by magnetization dynamics, for both metallic and insulating ferromagnets. As for the case of a metallic ferromagnet, a simple quantum mechanical picture was developed using a unitary transformation to diagonalize the time-dependent sd exchange interaction. The problem of dynamic magnetization is thereby mapped to the one with static magnetization and off-diagonal spin gauge field, which mixes the electron spin. In the slowly varying limit, the spin gauge field becomes static, and the conventional spin pumping formula is derived simply by evaluating the spin accumulation formed in the normal metal as a result of interface hopping. The effect of interface spin-orbit interaction was discussed. A rigorous field theoretical derivation was also presented, and the enhancement of spin damping (Gilbert damping) in the ferromagnet as a result of spin pumping effect was discussed. The case of an insulating ferromagnet was studied based on a model where the spin current is driven locally by the interface exchange interaction as a result of magnetic proximity effect. The dominant contribution turns out to be the one proportional to $\dot{\boldsymbol{n}}$, while the magnon contribution leads to $\boldsymbol{n}\times\dot{\boldsymbol{n}}$, whose amplitude depends linearly on the temperature. Our analysis clearly demonstrates the difference in the spin current generation mechanism for metallic and insulating ferromagnets. The influence of atomic-scale interface structure on the spin pumping effect is an open and urgent issue, in particular for the case of ferrimagnetic insulators which have two sublattice magnetic moments.

ACKNOWLEDGMENTS

G.T. thanks H. Kohno, C. Uchiyama, K. Hashimoto, and A. Shitade for valuable discussions. S.M. thanks the Center for Spintronics Network (CSRN) for supporting collaboration works. This work was supported by a Grant-in-Aid for Exploratory Research (Grant No.16K13853) and a Grant-in-Aid for Scientific Research (B) (Grant No. 17H02929) from the Japan Society for the Promotion of Science, and a Grant-in-Aid for Scientific Research on Innovative Areas (Grant No. 26103006) from The Ministry of Education, Culture, Sports, Science and Technology (MEXT), Japan.

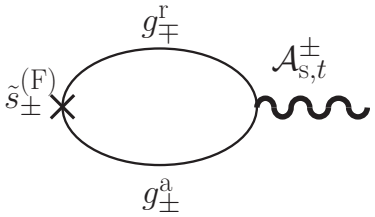

FIG. 11. Feynman diagram for electron spin density of ferromagnet induced by magnetization dynamics (represented by spin gauge field $\mathcal{A}_s$) neglecting the effect of normal metal. The amplitude is essentially given by the spin-flip correlation function $\chi_\pm$ [Eq. (A3)].

APPENDIX A: SPIN DENSITY INDUCED BY MAGNETIZATION DYNAMICS IN F

Let us here calculate the spin density in a ferromagnet induced by magnetization dynamics neglecting the effect of interface, $H_{\rm I}$. (Effects of $H_{\rm I}$ are discussed in Sec. V.)

In the rotated frame, the spin density in F pumped by the spin gauge field is therefore (diagrams shown in Fig. 11)

$$\begin{aligned}\tilde{s}^{(\rm F)}_{\alpha}(\boldsymbol{k},\boldsymbol{k}') &\equiv -i\int\frac{d\omega}{2\pi}\mathrm{tr}[\sigma_\alpha\delta G^<(\boldsymbol{k},\boldsymbol{k}',\omega)]\\ &= -i\int\frac{d\omega}{2\pi}\sum_{\boldsymbol{k}''}(f_{\boldsymbol{k}''+}-f_{\boldsymbol{k}''-})\sum_{\pm}(\pm)\mathcal{A}^{\pm}_{{\rm s},t}\mathrm{tr}[\sigma_\alpha g^{\rm r}(\boldsymbol{k},\boldsymbol{k}'',\omega)\sigma_\mp g^{\rm a}(\boldsymbol{k}'',\boldsymbol{k}',\omega)]\\ &= \begin{cases}\mp i\int\frac{d\omega}{2\pi}\sum_{\boldsymbol{k}''}(f_{\boldsymbol{k}''+}-f_{\boldsymbol{k}''-})\mathcal{A}^{\pm}_{{\rm s},t}g^{\rm r}_{\mp}(\boldsymbol{k},\boldsymbol{k}'',\omega)g^{\rm a}_{\pm}(\boldsymbol{k}'',\boldsymbol{k}',\omega) & (\alpha=\pm)\\ 0 & (\alpha=z)\end{cases}.\end{aligned}\tag{A1}$$

Let us here neglect the effects of interface in discussing the spin polarization of F electrons, then the Green's functions are translationally invariant, i.e., $g^a(\boldsymbol{k},\boldsymbol{k}')=\delta_{\boldsymbol{k},\boldsymbol{k}'}g^a(\boldsymbol{k})$ $(a={\rm r,a})$. Using the explicit form of the free Green's function, $g^{\rm a}_\sigma(\boldsymbol{k},\omega)=\frac{1}{\omega-\epsilon_{\boldsymbol{k},\sigma}-i0}$, and

$$\int\frac{d\omega}{2\pi}g^{\rm r}_{\mp}(\boldsymbol{k},\boldsymbol{k}'',\omega)g^{\rm a}_{\pm}(\boldsymbol{k}'',\boldsymbol{k}',\omega)=\frac{i}{\epsilon_{\boldsymbol{k},\pm}-\epsilon_{\boldsymbol{k},\mp}+i0},\tag{A2}$$

the spin density in the rotated frame then reduces to

$$\tilde{s}^{(\rm F)}_{\pm}(\boldsymbol{k})=-\mathcal{A}^{\pm}_{{\rm s},t}\chi_{\pm},\tag{A3}$$

where

$$\chi_{\pm}\equiv-\sum_{\boldsymbol{k}}\frac{f_{\boldsymbol{k},\pm}-f_{\boldsymbol{k},\mp}}{\epsilon_{\boldsymbol{k},\pm}-\epsilon_{\boldsymbol{k},\mp}+i0}\tag{A4}$$

is the spin correlation function with spin flip, $+i0$ meaning an infinitesimal positive imaginary part. Since we focus on the adiabatic limit and spatially uniform magnetization, the correlation function is at zero momentum and frequency transfer. We thus easily see that

$$\chi_{\pm}=\frac{n_+-n_-}{2M},\tag{A5}$$

where $n_\pm=\sum_{\boldsymbol{k}}f_{\boldsymbol{k}\pm}$ is the spin-resolved electron density.

The spin polarization of Eq. (A3) in the rotated frame is proportional to $\mathcal{A}^{\perp}_{{\rm s},t}$, and represents a renormalization of total spin in F. In fact, it corresponds in the laboratory frame to $\boldsymbol{s}^{(\rm F)}\propto\boldsymbol{n}\times\dot{\boldsymbol{n}}$, and exerts a torque proportional to $\dot{\boldsymbol{n}}$ on $\boldsymbol{n}$.

It may appear from Eq. (A5) that a damping of spin, i.e., a torque proportional to $\boldsymbol{n}\times\dot{\boldsymbol{n}}$, arises when the imaginary part for the Green's function becomes finite, because $\frac{1}{M}$ is replaced by $\frac{1}{M\mp i\eta_{\rm i}}$, where $\eta_{\rm i}$ is the imaginary part. This is not always the case. For example, nonmagnetic impurities introduce a finite imaginary part inversely proportional to the elastic lifetime (τ), $\frac{i}{2\tau}$. They should not, however, cause damping of spin. The solution to this apparent controversy is that Eq. (A1) is not enough to discuss damping even including lifetime. In fact, there is an additional process called vertex correction contributing to the lesser Green's function, and it gives rise to the same order of small correction as the lifetime does, and the sum of the two contributions vanishes. Similarly, we expect damping does not arise from the spin-conserving component of spin gauge field, $\mathcal{A}^{z}_{{\rm s},t}$. This is indeed true as we explicitly demonstrate in Appendix B. We shall show in Sec. V that damping arises from the spin-flip components of the self-energy.

APPENDIX B: EFFECT OF SPIN-CONSERVING SPIN GAUGE FIELD ON SPIN DENSITY

Here we calculate the contribution of spin-conserving spin gauge field, $\mathcal{A}^{z}_{{\rm s},t}$, on the interface effects of spin density in F. It turns out that a spin-conserving spin gauge field combined with interface effects does not induce damping. This result is consistent with a naive expectation that only the nonadiabatic components of spin current should contribute to damping.

The contribution to the lesser Green's function in F from the interface hopping (lowest, the second order in the hopping) at the linear order in the spin gauge field reads (diagramatically shown in Fig. 12)

$$\begin{aligned}\delta G^< &= \delta G^<_{\rm (a)}+\delta G^<_{\rm (b)}+\delta G^<_{\rm (c)},\\ \delta G^<_{\rm (a)} &= g^{\rm r}(\boldsymbol{\mathcal{A}}_{{\rm s},t}\cdot\boldsymbol{\sigma})g^{\rm r}\Sigma^{\rm r}_0g^< + g^{\rm r}(\boldsymbol{\mathcal{A}}_{{\rm s},t}\cdot\boldsymbol{\sigma})g^{\rm r}\Sigma^<_0g^{\rm a}\\ &\quad + g^{\rm r}(\boldsymbol{\mathcal{A}}_{{\rm s},t}\cdot\boldsymbol{\sigma})g^<\Sigma^{\rm a}_0g^{\rm a} + g^<(\boldsymbol{\mathcal{A}}_{{\rm s},t}\cdot\boldsymbol{\sigma})g^{\rm a}\Sigma^{\rm a}_0g^{\rm a},\\ \delta G^<_{\rm (b)} &= g^{\rm r}\Sigma^{\rm r}_0g^{\rm r}(\boldsymbol{\mathcal{A}}_{{\rm s},t}\cdot\boldsymbol{\sigma})g^< + g^{\rm r}\Sigma^<_0g^<(\boldsymbol{\mathcal{A}}_{{\rm s},t}\cdot\boldsymbol{\sigma})g^{\rm a}\\ &\quad + g^{\rm r}\Sigma^{\rm a}_0g^{\rm a}(\boldsymbol{\mathcal{A}}_{{\rm s},t}\cdot\boldsymbol{\sigma})g^{\rm a} + g^<\Sigma^{\rm a}_0g^{\rm a}(\boldsymbol{\mathcal{A}}_{{\rm s},t}\cdot\boldsymbol{\sigma})g^{\rm a},\\ \delta G^<_{\rm (c)} &= g^{\rm r}\Sigma^{\rm r}g^< + g^{\rm r}\Sigma^<g^{\rm a} + g^<\Sigma^{\rm a}g^{\rm a}.\end{aligned}\tag{B1}$$

Here,

$$\begin{aligned}\Sigma^a &\equiv \tilde{t}U^{-1}g^a_{\rm N}U\tilde{t}^\dagger\quad(a={\rm a,r,<}),\\ \Sigma^a_0 &\equiv \tilde{t}g^a_{\rm N}\end{aligned}\tag{B2}$$

are the self-energy due to the interface hopping, where Σ^a is the full self-energy including the time-dependent unitary matrix U, which includes the spin gauge field. Σ^a_0 is the

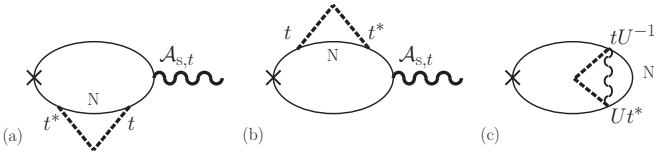

FIG. 12. Diagrammatic representation of the contribution to the lesser Green's function for F electron arising from the interface hopping (represented by t and t^*) and spin gauge field ($\mathcal{A}_{{\rm s},t}$). The diagram (c) includes the spin gauge field implicitly in unitary matrices U and U^{-1}.

contribution of Σ^a with the spin gauge field neglected. We here focus on the contribution of the adiabatic (z) component, $\mathcal{A}^z_{s,t}$. Using $g^< = F(g^a - g^r)$ for F (F is a 2×2 matrix of the spin-polarized Fermi distribution function) and $g^<_N = f_N(g^a_N - g^r_N)$ and noting that all the angular frequencies of the Green's function are equal, we obtain

$$\delta G^<_{(a)} + \delta G^<_{(b)} \simeq \mathcal{A}^z_{s,t}\sigma_z\left\{-2F\left[(g^r)^3\Sigma^r_0 - (g^a)^3\Sigma^a_0\right] - (F - f_N)[(g^r)^2 g^a + g^r(g^a)^2]\left(\Sigma^a_0 - \Sigma^r_0\right)\right\}. \tag{B3}$$

The contribution $\delta G^<_{(c)}$ is calculated noting that

$$\tilde{t}U^{-1}g^a_N U\tilde{t}^\dagger = g^a_N\tilde{t}\tilde{t}^\dagger - \frac{dg^a_N}{d\omega}\tilde{t}(\boldsymbol{\mathcal{A}}_{s,t}\cdot\boldsymbol{\sigma})\tilde{t}^\dagger + O((\boldsymbol{\mathcal{A}}_{s,t})^2). \tag{B4}$$

The linear contribution with respect to the z component of the gauge field turns out to be

$$\delta G^<_{(c)} \simeq \mathcal{A}^z_{s,t}\sigma_z\left\{F\left[(g^r)^2\frac{\partial}{\partial\omega}\Sigma^r_0 - (g^a)^2\frac{\partial}{\partial\omega}\Sigma^a_0\right] + (F - f_N)g^r g^a\frac{\partial}{\partial\omega}\left(\Sigma^a_0 - \Sigma^r_0\right)\right\}. \tag{B5}$$

We therefore obtain the effect of spin-conserving gauge field as

$$\delta G^< = \mathcal{A}^z_{s,t}\sigma_z\frac{\partial}{\partial\omega}\left\{F\left[(g^r)^2\Sigma^r_0 - (g^a)^2\Sigma^a_0\right] + (F - f_N)g^r g^a\left(\Sigma^a_0 - \Sigma^r_0\right)\right\}, \tag{B6}$$

which vanishes after integration over ω. Therefore the contribution from the spin-conserving gauge field and interface hopping vanishes in the spin density, leaving the damping unaffected.

APPENDIX C: DERIVATION OF EQ. (72)

We show here the details of the calculation of the induced spin density in the ferromagnetic metal, diagrammatically represented in Fig. 8. Writing the spatial and temporal positions explicitly, the self-energy of F electrons arising from the hopping to N region reads ($\boldsymbol{r}_1$ and $\boldsymbol{r}_2$ are in F)

$$\Sigma^a(\boldsymbol{r}_1,\boldsymbol{r}_2,t_1,t_2) = \int_{I_N} d^3r'_1\int_{I_N} d^3r'_2\tilde{t}(\boldsymbol{r}_1,\boldsymbol{r}'_1)U^{-1}(t_1)g^a_N(\boldsymbol{r}'_1,\boldsymbol{r}'_2,t_1-t_2)U(t_2)\tilde{t}^\dagger(\boldsymbol{r}_2,\boldsymbol{r}'_2), \tag{C1}$$

where $a = $ r,a, $<$. We assume the Green's function in N region is spin-independent, i.e., we neglect higher-order contributions of hopping. Moreover, we treat the hopping to occur only at the interface, i.e., at $x = 0$. The self-energy is then represented as

$$\Sigma^a(\boldsymbol{r}_1,\boldsymbol{r}_2,t_1,t_2) = a^2\delta(x_1)\delta(x_2)\tilde{t}U^{-1}(t_1)U(t_2)\tilde{t}^\dagger\sum_{\boldsymbol{k}} g^a_N(\boldsymbol{k},t_1-t_2), \tag{C2}$$

where a is the interface thickness, which we assume to be the order of the lattice constant. The diagrammatic representations of Eqs. (68) and (C1) are in Fig. 8. Expanding the matrix using a spin gauge field as $U^{-1}(t_1)U(t_2) = 1 - i(t_1-t_2)\mathcal{A}_{s,t} + O((\mathcal{A}_{s,t})^2)$, we obtain the gauge field contribution of the self-energy as

$$\begin{aligned}\Sigma^a(\boldsymbol{r}_1,\boldsymbol{r}_2,t_1,t_2) &= a^2\delta(x_1)\delta(x_2)\int\frac{d\omega}{2\pi}\frac{de^{-i\omega(t_1-t_2)}}{d\omega}\tilde{t}A_{s,t}\tilde{t}^\dagger\sum_{\boldsymbol{k}} g^a_N(\boldsymbol{k},\omega)\\ &= -a^2\delta(x_1)\delta(x_2)\int\frac{d\omega}{2\pi}e^{-i\omega(t_1-t_2)}\tilde{t}A_{s,t}\tilde{t}^\dagger\sum_{\boldsymbol{k}}\frac{d}{d\omega}g^a_N(\boldsymbol{k},\omega).\end{aligned} \tag{C3}$$

The linear contribution of the lesser component of the off-diagonal self-energy is

$$\begin{aligned}G^<(\boldsymbol{r},t,\boldsymbol{r}',t) &= g^r\Sigma^r g^a + g^r\Sigma^< g^a + g^<\Sigma^a g^a\\ &= a^2\int\frac{d\omega}{2\pi}\sum_{\boldsymbol{k}}\Bigg[g^r(\boldsymbol{r},\omega)\frac{dg^r_N(\boldsymbol{k},\omega)}{d\omega}\tilde{t}A_{s,t}\tilde{t}^\dagger g^<(-\boldsymbol{r},\omega)\\ &\quad + g^r(\boldsymbol{r},\omega)\frac{dg^<_N(\boldsymbol{k},\omega)}{d\omega}\tilde{t}A_{s,t}\tilde{t}^\dagger g^a(-\boldsymbol{r},\omega) + g^<(\boldsymbol{r},\omega)\frac{dg^a_N(\boldsymbol{k},\omega)}{d\omega}\tilde{t}A_{s,t}\tilde{t}^\dagger g^a(-\boldsymbol{r},\omega)\Bigg].\end{aligned} \tag{C4}$$

For a finite distance from the interface r, the dominant contribution arises from the terms containing both $g^r(\boldsymbol{r},\omega)$ and $g^a(-\boldsymbol{r},\omega)$, as they do not contain a rapid oscillation like $e^{i(k_{F+}+k_{F-})r}$ and $e^{2ik_{F\sigma}r}$. Using an approximation $\sum_{\boldsymbol{k}} g^r_N(\boldsymbol{k},\omega) \sim -i\pi\nu_N$ and partial integration with respect to ω, Eq. (C4) finally reduces to Eq. (72).

APPENDIX D: MAGNON REPRESENTATION OF SPIN BERRY'S PHASE TERM

Here we derive the expression for the spin Berry's phase term of the Lagrangian (94) in terms of a magnon operator. The time integral of the term is written by introducing an artificial variable u as [56]

$$\int dt L_{\rm B} = S\int dt\dot{\phi}(\cos\theta - 1) = S^{-2}\int dt\int_0^1 du\boldsymbol{S}\cdot(\partial_t\boldsymbol{S}\times\partial_u\boldsymbol{S}), \tag{D1}$$

where $\boldsymbol{S}(t,u)$ is extended to a function of t and u, but only $\boldsymbol{S}(t,u=1)$ is physical. Noting that the unitary transformation matrix element of Eq. (96) is written as

$$U_{ij} = (\boldsymbol{e}_j)_i, \tag{D2}$$

where $\boldsymbol{r}_1 \equiv \boldsymbol{e}_\theta$, $\boldsymbol{e}_2 \equiv \boldsymbol{e}_\phi$ and $\boldsymbol{e}_3 \equiv \boldsymbol{n}$, we obtain

$$\boldsymbol{S}\cdot(\partial_t\boldsymbol{S}\times\partial_u\boldsymbol{S}) = \widetilde{\boldsymbol{S}}\cdot[(\partial_t + iA_{U,t})\widetilde{\boldsymbol{S}}\times(\partial_u + iA_{U,u})\widetilde{\boldsymbol{S}})]. \tag{D3}$$

Evaluating to the second order in the magnon operators, we have

$$\partial_t\widetilde{\boldsymbol{S}}\times\partial_u\widetilde{\boldsymbol{S}} = 2i\gamma\hat{\boldsymbol{z}}[(\partial_u b^\dagger)(\partial_t b) - (\partial_t b^\dagger)(\partial_u b)]. \tag{D4}$$

Using the explicit form of $A_{U,\mu}$, the gauge field contribution is

$$\partial_u\widetilde{\boldsymbol{S}}\cdot[\widetilde{\boldsymbol{S}}\times iA_{U,t}\widetilde{\boldsymbol{S}})] = S^2\gamma[(\partial_u b^\dagger)(-\sin\theta\dot{\phi} + i\dot{\theta}) + (\partial_u b)(-\sin\theta\dot{\phi} - i\dot{\theta})] - 2S\gamma^2\cos\theta(\partial_t\phi)\partial_u(b^\dagger b). \tag{D5}$$

The terms linear in the boson operators vanish by the equation of motion, and the second-order contribution is

$$\begin{aligned}\boldsymbol{S}\cdot(\partial_t\boldsymbol{S}\times\partial_u\boldsymbol{S}) = 2S\gamma^2\{&i\partial_u[b^\dagger(\partial_t b) - (\partial_t b^\dagger)b] - \partial_u[\cos\theta(\partial_t\phi)b^\dagger b] + \partial_t[\cos\theta(\partial_u\phi)b^\dagger b]\\ &+ \sin\theta((\partial_t\theta)(\partial_u\phi) - (\partial_u\theta)(\partial_t\phi))b^\dagger b\}.\end{aligned} \tag{D6}$$

Integrating over t and u, the total derivative with respect to t of Eq. (D6) vanishes, resulting in

$$\int dt\int_0^1 du\boldsymbol{S}\cdot(\partial_t\boldsymbol{S}\times\partial_u\boldsymbol{S}) = 2S\gamma^2\int dt\{i[b^\dagger(\partial_t b) - (\partial_t b^\dagger)b] - \cos\theta(\partial_t\phi)b^\dagger b + \sin\theta((\partial_t\theta)(\partial_u\phi) - (\partial_u\theta)(\partial_t\phi))b^\dagger b\}. \tag{D7}$$

The last term of Eq. (D7) represents the renormalization of spin Berry's phase term, i.e., the effect $S \to S - b^\dagger b$, which we neglect below. The Lagrangian for magnons thus reads

$$L_{\rm m} = 2S\gamma^2\int d^3r i\big[b^\dagger\big(\partial_t + i\mathcal{A}^z_{{\rm s},t}\big)b - b^\dagger\big(\overleftarrow{\partial}_t - i\mathcal{A}^z_{{\rm s},t}\big)\big)b\big], \tag{D8}$$

namely, magnons interacts with the adiabatic component of the spin gauge field, $\mathcal{A}^z_{{\rm s},t}$.

APPENDIX E: DERIVATION OF EQS. (120) AND (121)

For the self-energy type of the Green's functions, depending on two times as $g(t_1 - t_2)\mathcal{D}(t_1 - t_2)$ [Eq. (117)], the real-time components are written as (suppressing time and suffix of N) (see Appendix F)

$$\begin{aligned}[g(t_1 - t_2)\mathcal{D}(t_1 - t_2)]^{\rm r} &= g^{\rm r}\mathcal{D}^< + g^>\mathcal{D}^{\rm r} = g^<\mathcal{D}^{\rm r} + g^{\rm r}\mathcal{D}^>,\\ [g(t_1 - t_2)\mathcal{D}(t_1 - t_2)]^{\rm a} &= g^{\rm a}\mathcal{D}^> + g^<\mathcal{D}^{\rm a} = g^{\rm a}\mathcal{D}^< + g^>\mathcal{D}^{\rm a},\\ [g(t_1 - t_2)\mathcal{D}(t_1 - t_2)]^< &= g^<\mathcal{D}^<.\end{aligned} \tag{E1}$$

The Green's function $\widetilde{\mathcal{D}}$ is that of a composite field $\mathcal{B}_\alpha$ defined in Eq. (115), and is decomposed to the elementary magnon Green's function D as

$$\widetilde{\mathcal{D}}_\gamma(\boldsymbol{r}_1,t_1,\boldsymbol{r}_2,t_2) = [\boldsymbol{\Phi}^\dagger(t_1)\times\boldsymbol{\Phi}(t_2)]_\gamma D(\boldsymbol{r}_1,t_1,\boldsymbol{r}_2,t_2) - [\boldsymbol{\Phi}^\dagger(t_2)\times\boldsymbol{\Phi}(t_1)]_\gamma D(\boldsymbol{r}_2,t_2,\boldsymbol{r}_1,t_1), \tag{E2}$$

where

$$D(\boldsymbol{r}_1,t_1,\boldsymbol{r}_2,t_2) \equiv -i\langle T_C b(\boldsymbol{r}_1,t_1)b^\dagger(\boldsymbol{r}_2,t_2)\rangle. \tag{E3}$$

The spin-dependent factor in Eq. (E2) is calculated for adiabatic dynamics as

$$\boldsymbol{\Phi}^\dagger(t_1)\times\boldsymbol{\Phi}(t_2) = 2i\boldsymbol{n}(t_1) + (t_2 - t_1)[\boldsymbol{\Psi} + i\dot{\boldsymbol{n}}] + O((\partial_t)^2), \tag{E4}$$

where

$$\boldsymbol{\Psi} \equiv 2\cos\theta\dot{\phi}\boldsymbol{n} + \boldsymbol{n}\times\dot{\boldsymbol{n}}. \tag{E5}$$

The real-time Green's functions are therefore $[D(1,2) \equiv D(\boldsymbol{r}_1,t_1,\boldsymbol{r}_2,t_2)]$

$$\begin{aligned}\widetilde{\mathcal{D}}^{<}_{\gamma}(\boldsymbol{r}_1,t_1,\boldsymbol{r}_2,t_2) &= 2i\boldsymbol{n}(t_1)[D^{<}(\boldsymbol{r}_1,t_1,\boldsymbol{r}_2,t_2) - D^{>}(\boldsymbol{r}_2,t_2,\boldsymbol{r}_1,t_1)] + (t_2-t_1)\{\boldsymbol{\Psi}[D^{<}(\boldsymbol{r}_1,t_1,\boldsymbol{r}_2,t_2) + D^{>}(\boldsymbol{r}_2,t_2,\boldsymbol{r}_1,t_1)] \\ &\quad + i\dot{\boldsymbol{n}}[D^{<}(\boldsymbol{r}_1,t_1,\boldsymbol{r}_2,t_2) - D^{>}(\boldsymbol{r}_2,t_2,\boldsymbol{r}_1,t_1)]\}, \\ \widetilde{\mathcal{D}}^{\mathrm{r}}_{\gamma}(1,2) &= \theta(t_1-t_2)\big(\widetilde{\mathcal{D}}^{<}_{\gamma}(1,2) - \widetilde{\mathcal{D}}^{>}_{\gamma}(1,2)\big), \quad \widetilde{\mathcal{D}}^{\mathrm{a}}_{\gamma}(1,2) = -\theta(t_2-t_1)\epsilon_{\alpha\beta\gamma}(\mathcal{D}^{<}_{\alpha\beta}(1,2) - \mathcal{D}^{>}_{\alpha\beta}(1,2)),\end{aligned} \tag{E6}$$

and $\widetilde{\mathcal{D}}^{<}_{\gamma}$ is obtained by exchanging $<$ and $>$ in $\widetilde{\mathcal{D}}^{<}_{\gamma}$. Elementary Green's functions are calculated as

$$D^{<}(\boldsymbol{r}_1,t_1,\boldsymbol{r}_2,t_2) = -i\sum_{\boldsymbol{q}} e^{i\boldsymbol{q}\cdot(\boldsymbol{r}_1-\boldsymbol{r}_2)} n_{\boldsymbol{q}} e^{-i\omega_{\boldsymbol{q}}(t_1-t_2)}, \quad D^{>}(\boldsymbol{r}_1,t_1,\boldsymbol{r}_2,t_2) = -i\sum_{\boldsymbol{q}} e^{i\boldsymbol{q}\cdot(\boldsymbol{r}_1-\boldsymbol{r}_2)}(n_{\boldsymbol{q}}+1) e^{-i\omega_{\boldsymbol{q}}(t_1-t_2)}, \tag{E7}$$

where $\omega_{\boldsymbol{q}}$ is the magnon energy and $n_{\boldsymbol{q}} \equiv \frac{1}{e^{\beta\omega_{\boldsymbol{q}}}-1}$. In our model, the interface is atomically flat and has an infinite area, and thus $\boldsymbol{r}_i (i = 1,2)$ are at $x = 0$. The Fourier components, defined as $(a = \mathrm{r},\mathrm{a},<,>)$

$$\widetilde{\mathcal{D}}^{a}_{\gamma}(x_1 = 0,t_1,x_2 = 0,t_2) \equiv \sum_{\boldsymbol{q}} \int \frac{d\Omega}{2\pi} e^{-i\Omega(t_1-t_2)} \widetilde{\mathcal{D}}^{a}_{\gamma}(\boldsymbol{q},\Omega), \tag{E8}$$

are calculated from Eq. (E6) as

$$\begin{aligned}\widetilde{\mathcal{D}}^{<}_{\gamma}(\boldsymbol{q},\Omega) &= -i\left\{2\boldsymbol{n}(D^{<}_{-} - D^{>}_{+}) + \frac{d}{d\Omega}\big[\boldsymbol{\Psi}(D^{<}_{-} + D^{>}_{+}) + i\dot{\boldsymbol{n}}(D^{<}_{-} - D^{>}_{+})\big]\right\}, \\ \widetilde{\mathcal{D}}^{\mathrm{r}}_{\gamma}(\boldsymbol{q},\Omega) &= -i\left\{2\boldsymbol{n}(D^{\mathrm{r}}_{-} + D^{\mathrm{r}}_{+}) + \frac{d}{d\Omega}\big[\boldsymbol{\Psi}(D^{\mathrm{r}}_{-} - D^{\mathrm{r}}_{+}) + i\dot{\boldsymbol{n}}(D^{\mathrm{r}}_{-} + D^{\mathrm{r}}_{+})\big]\right\}, \\ \widetilde{\mathcal{D}}^{\mathrm{a}}_{\gamma}(\boldsymbol{q},\Omega) &= -i\left\{2\boldsymbol{n}(D^{\mathrm{a}}_{-} + D^{\mathrm{a}}_{+}) + \frac{d}{d\Omega}\big[\boldsymbol{\Psi}(D^{\mathrm{a}}_{-} - D^{\mathrm{a}}_{+}) + i\dot{\boldsymbol{n}}(D^{\mathrm{a}}_{-} + D^{\mathrm{a}}_{+})\big]\right\},\end{aligned} \tag{E9}$$

where

$$\begin{aligned}D^{\mathrm{a}}_{\pm} &\equiv \frac{1}{\Omega \pm \omega_{\boldsymbol{q}} - i0}, \quad D^{\mathrm{r}}_{\pm} \equiv \frac{1}{\Omega \pm \omega_{\boldsymbol{q}} + i0} \\ D^{<}_{-} &\equiv n_{\boldsymbol{q}}(D^{\mathrm{a}}_{-} - D^{\mathrm{r}}_{-}), \quad D^{>}_{+} \equiv (1+n_{\boldsymbol{q}})(D^{\mathrm{a}}_{+} - D^{\mathrm{r}}_{+}).\end{aligned} \tag{E10}$$

The spin part of the Green's function, Eq. (118), is

$$\begin{aligned}G^{<}_{\mathrm{N},\gamma}(\boldsymbol{r},t,\boldsymbol{r}',t) = -\frac{SJ_{\mathrm{I}}^2}{2}\int\frac{d\omega}{2\pi}\int\frac{d\Omega}{2\pi}\sum_{\boldsymbol{k}\boldsymbol{k}'}\sum_{\boldsymbol{k}''\boldsymbol{q}}\big[&g^{\mathrm{r}}_{\mathrm{N},\boldsymbol{k}\omega}\big(\widetilde{\mathcal{D}}^{\mathrm{r}}_{\gamma}(\boldsymbol{q},\Omega)g^{>}_{\mathrm{N},\boldsymbol{k}'',\omega-\Omega} + \widetilde{\mathcal{D}}^{<}_{\gamma}(\boldsymbol{q},\Omega)g^{\mathrm{r}}_{\mathrm{N},\boldsymbol{k}'',\omega-\Omega}\big)g^{<}_{\mathrm{N},\boldsymbol{k}'\omega} \\ &+ g^{\mathrm{r}}_{\mathrm{N},\boldsymbol{k}\omega}\widetilde{\mathcal{D}}^{\mathrm{r}}_{\gamma}(\boldsymbol{q},\Omega)g^{>}_{\mathrm{N},\boldsymbol{k}'',\omega-\Omega}g^{\mathrm{a}}_{\mathrm{N},\boldsymbol{k}'\omega} + g^{<}_{\mathrm{N},\boldsymbol{k}\omega}\big(\widetilde{\mathcal{D}}^{\mathrm{a}}_{\gamma}(\boldsymbol{q},\Omega)g^{>}_{\mathrm{N},\boldsymbol{k}'',\omega-\Omega} + \widetilde{\mathcal{D}}^{<}_{\gamma}(\boldsymbol{q},\Omega)g^{\mathrm{a}}_{\mathrm{N},\boldsymbol{k}'',\omega-\Omega}\big)g^{\mathrm{a}}_{\mathrm{N},\boldsymbol{k}'\omega}\big].\end{aligned} \tag{E11}$$

The contribution surviving at long distance is the one containing $g^{\mathrm{r}}_{\mathrm{N},\omega}(\boldsymbol{r})$ and $g^{\mathrm{a}}_{\mathrm{N},\omega}(-\boldsymbol{r})$, obtaining Eq. (120), i.e.,

$$G^{<}_{\mathrm{N},\gamma}(\boldsymbol{r},t,\boldsymbol{r}',t) \simeq \int\frac{d\omega}{2\pi}\sum_{\boldsymbol{k}\boldsymbol{k}'} g^{\mathrm{r}}_{\mathrm{N},\boldsymbol{k}\omega}g^{\mathrm{a}}_{\mathrm{N},\boldsymbol{k}'\omega}e^{i\boldsymbol{k}\cdot\boldsymbol{r}}e^{-i\boldsymbol{k}'\cdot\boldsymbol{r}'}\widetilde{\Sigma}_{\mathrm{I},\gamma},$$

where

$$\begin{aligned}\widetilde{\Sigma}_{\mathrm{I},\gamma} \equiv -\frac{SJ_{\mathrm{I}}^2}{2}\int\frac{d\Omega}{2\pi}\sum_{\boldsymbol{k}''\boldsymbol{q}}\big[&\big(f_{\boldsymbol{k}'}\widetilde{\mathcal{D}}^{\mathrm{r}}_{\gamma}(\boldsymbol{q},\Omega) - f_{\boldsymbol{k}}\widetilde{\mathcal{D}}^{\mathrm{a}}_{\gamma}(\boldsymbol{q},\Omega)\big)(f_{\boldsymbol{k}''}-1)\big(g^{\mathrm{a}}_{\mathrm{N},\boldsymbol{k}'',\omega-\Omega} - g^{\mathrm{r}}_{\mathrm{N},\boldsymbol{k}'',\omega-\Omega}\big) \\ &+ \widetilde{\mathcal{D}}^{<}_{\gamma}(\boldsymbol{q},\Omega)\big(f_{\boldsymbol{k}'}g^{\mathrm{r}}_{\mathrm{N},\boldsymbol{k}'',\omega-\Omega} - f_{\boldsymbol{k}}g^{\mathrm{a}}_{\mathrm{N},\boldsymbol{k}'',\omega-\Omega} + f_{\boldsymbol{k}''}\big(g^{\mathrm{a}}_{\mathrm{N},\boldsymbol{k}'',\omega-\Omega} - g^{\mathrm{r}}_{\mathrm{N},\boldsymbol{k}'',\omega-\Omega}\big)\big)\big].\end{aligned} \tag{E12}$$

We focus on the pumped contribution, containing a derivative with respect to Ω in Eq. (E9). The result is, using partial integration with respect to Ω ($\widetilde{\boldsymbol{\Sigma}}_{\mathrm{I}}$ is a vector representation of $\widetilde{\Sigma}_{\mathrm{I},\gamma}$),

$$\begin{aligned}\widetilde{\boldsymbol{\Sigma}}_{\mathrm{I}} \simeq -i\frac{SJ_{\mathrm{I}}^2}{2}\int\frac{d\Omega}{2\pi}\sum_{\boldsymbol{k}''\boldsymbol{q}}\Big\{&(f_{\boldsymbol{k}''}-1)\frac{d}{d\Omega}\big(g^{\mathrm{a}}_{\mathrm{N},\boldsymbol{k}'',\omega-\Omega} - g^{\mathrm{r}}_{\mathrm{N},\boldsymbol{k}'',\omega-\Omega}\big)(f_{\boldsymbol{k}'}[\boldsymbol{\Psi}(D^{\mathrm{r}}_{-} - D^{\mathrm{r}}_{+}) + i\dot{\boldsymbol{n}}(D^{\mathrm{r}}_{-} + D^{\mathrm{r}}_{+})] \\ &- f_{\boldsymbol{k}}[\boldsymbol{\Psi}(D^{\mathrm{a}}_{-} - D^{\mathrm{a}}_{+}) + i\dot{\boldsymbol{n}}(D^{\mathrm{a}}_{-} + D^{\mathrm{a}}_{+})]) + [\boldsymbol{\Psi}(D^{<}_{-} + D^{>}_{+}) \\ &+ i\dot{\boldsymbol{n}}(D^{<}_{-} - D^{>}_{+})]\frac{d}{d\Omega}\big((f_{\boldsymbol{k}''} - f_{\boldsymbol{k}})g^{\mathrm{a}}_{\mathrm{N},\boldsymbol{k}'',\omega-\Omega} - (f_{\boldsymbol{k}''} - f_{\boldsymbol{k}'})g^{\mathrm{r}}_{\mathrm{N},\boldsymbol{k}'',\omega-\Omega}\big)\Big\}.\end{aligned} \tag{E13}$$

Using $\frac{d}{d\Omega} g^{\rm a}_{\boldsymbol{k}'',\omega-\Omega} = (g^{\rm a}_{\boldsymbol{k}'',\omega})^2 + O(\Omega)$ and an approximation, we obtain $\sum_{\boldsymbol{k}''}(g^{\rm a}_{\boldsymbol{k}'',\omega})^2 \simeq -\pi i \frac{\nu}{2\epsilon_F}$,

$$\widetilde{\boldsymbol{\Sigma}}_{\rm I} \simeq \frac{\pi\nu}{\epsilon_F}\frac{SJ_{\rm I}^2}{2}\int\frac{d\Omega}{2\pi}\sum_{\boldsymbol{q}\boldsymbol{k}''}\Bigg(\boldsymbol{\Psi}\Big\{(f_{\boldsymbol{k}''}-1)[f_{\boldsymbol{k}'}(D^{\rm r}_- - D^{\rm r}_+) - f_{\boldsymbol{k}}(D^{\rm a}_- - D^{\rm a}_+)] + \frac{1}{2}(2f_{\boldsymbol{k}''} - f_{\boldsymbol{k}} - f_{\boldsymbol{k}'})(D^{<}_- + D^{>}_+)\Big\}$$
$$+ i\dot{\boldsymbol{n}}\Big\{(f_{\boldsymbol{k}''}-1)[f_{\boldsymbol{k}'}(D^{\rm r}_- + D^{\rm r}_+) - f_{\boldsymbol{k}}(D^{\rm a}_- + D^{\rm a}_+)] + \frac{1}{2}(2f_{\boldsymbol{k}''} - f_{\boldsymbol{k}} - f_{\boldsymbol{k}'})(D^{<}_- - D^{>}_+)\Big\}\Bigg). \tag{E14}$$

As argued for Eq. (106), only the imaginary part of self-energy contributes to the induced spin current, as the real part, the shift of the chemical potential, is compensated by redistribution of electrons. We therefore obtain Eq. (121).

We further note that the component of $\boldsymbol{\Psi}$ proportional to $\boldsymbol{n}$ [Eq. (E5)] does not contribute to the current generation, as a result of gauge invariance. (In other words, the contribution cancels with the one arising from the effective gauge field for magnons).

APPENDIX F: DECOMPOSITION OF CONTOUR-ORDERED SELF-ENERGY

Here we derive the decomposition formula for the self-energy in Eq. (E1). Obviously, we have

$$[g\mathcal{D}]^{<} = g^{<}\mathcal{D}^{<}. \tag{F1}$$

The retarded component is defined as

$$[g\mathcal{D}]^{\rm r} \equiv [g\mathcal{D}]^{\rm t} - [g\mathcal{D}]^{<}, \tag{F2}$$

where the time-ordered one is written as

$$[g(t_1-t_2)\mathcal{D}(t_1-t_2)]^{\rm t} \equiv \theta(t_1-t_2)g^{>}\mathcal{D}^{>} + \theta(t_2-t_1)g^{<}\mathcal{D}^{<} = g^{\rm r}\mathcal{D}^{\rm r} + g^{\rm r}\mathcal{D}^{<} + g^{<}\mathcal{D}^{\rm r} + g^{<}\mathcal{D}^{<}. \tag{F3}$$

We thus obtain

$$[g\mathcal{D}]^{\rm r} = g^{\rm r}\mathcal{D}^{\rm r} + g^{\rm r}\mathcal{D}^{<} + g^{<}\mathcal{D}^{\rm r}. \tag{F4}$$

Noting that $g^{\rm r}\mathcal{D}^{\rm a} = 0$, we can write it as

$$[g\mathcal{D}]^{\rm r} = g^{\rm r}\mathcal{D}^{<} + g^{>}\mathcal{D}^{\rm r} = g^{<}\mathcal{D}^{\rm r} + g^{\rm r}\mathcal{D}^{>}. \tag{F5}$$

The advanced component is similarly written as

$$[g\mathcal{D}]^{\rm a} = -g^{\rm a}\mathcal{D}^{\rm a} + g^{\rm a}\mathcal{D}^{<} + g^{<}\mathcal{D}^{\rm a} = g^{\rm a}\mathcal{D}^{>} + g^{<}\mathcal{D}^{\rm a} = g^{\rm a}\mathcal{D}^{<} + g^{>}\mathcal{D}^{\rm a}. \tag{F6}$$

[1] E. Saitoh, M. Ueda, H. Miyajima, and G. Tatara, Appl. Phys. Lett. **88**, 182509 (2006).
[2] Y. Tserkovnyak, A. Brataas, and G. E. W. Bauer, Phys. Rev. Lett. **88**, 117601 (2002).
[3] M. V. Moskalets, *Scattering Matrix Approach to Non-Stationary Quantum Transport* (Imperial College Press, 2012).
[4] M. Büttiker, H. Thomas, and A. Prtre, Z. Phys. B **94**, 133 (1994).
[5] P. W. Brouwer, Phys. Rev. B **58**, R10135 (1998).
[6] G. Tatara and H. Kohno, Phys. Rev. B **67**, 113316 (2003).
[7] G. Tatara, H. Kohno, and J. Shibata, Phys. Rep. **468**, 213 (2008).
[8] Y. Kang *et al.*, Chin. Phys. B **26**, 047272 (2017).
[9] V. K. Dugaev, P. Bruno, B. Canals, and C. Lacroix, Phys. Rev. B **72**, 024456 (2005).
[10] R. H. Silsbee, A. Janossy, and P. Monod, Phys. Rev. B **19**, 4382 (1979).
[11] L. Berger, Phys. Rev. B **54**, 9353 (1996).
[12] S. Mizukami, Y. Ando, and T. Miyazaki, Jpn. J. Appl. Phys. **40**, 580 (2001).
[13] E. Šimánek and B. Heinrich, Phys. Rev. B **67**, 144418 (2003).
[14] E. Šimánek, Phys. Rev. B **68**, 224403 (2003).
[15] K. Chen and S. Zhang, Phys. Rev. Lett. **114**, 126602 (2015).
[16] G. Tatara, Phys. Rev. B **94**, 224412 (2016).
[17] D. S. Fisher and P. A. Lee, Phys. Rev. B **23**, 6851 (1981).
[18] A. Takeuchi and G. Tatara, J. Phys. Soc. Jpn. **77**, 074701 (2008).
[19] K. Hosono, A. Takeuchi, and G. Tatara, J. Phys.: Conf. Ser. **150**, 022029 (2009).
[20] H. Adachi, J.-i. Ohe, S. Takahashi, and S. Maekawa, Phys. Rev. B **83**, 094410 (2011).
[21] J. J. Sakurai, *Modern Quantum Mechanics* (Addison Wesley, 1994).
[22] K. Xia, P. J. Kelly, G. E. W. Bauer, A. Brataas, and I. Turek, Phys. Rev. B **65**, 220401 (2002).
[23] M. Zwierzycki, Y. Tserkovnyak, P. J. Kelly, A. Brataas, and G. E. W. Bauer, Phys. Rev. B **71**, 064420 (2005).
[24] K. Hashimoto, G. Tatara, and C. Uchiyama, arXiv:1706.00583.
[25] G. Tatara, H. Kohno, J. Shibata, Y. Lemaho, and K.-J. Lee, J. Phys. Soc. Jpn. **76**, 054707 (2007).
[26] G. Tatara, arXiv:1612.09019.
[27] G. Tatara, J. Phys. Soc. Jpn. **69**, 2969 (2000).
[28] G. Tatara, Int. J. Mod. Phys. B. **15**, 321 (2001).
[29] G. Tatara and H. Kohno, Phys. Rev. Lett. **92**, 086601 (2004).
[30] J.-C. Rojas-Sánchez, N. Reyren, P. Laczkowski, W. Savero, J.-P. Attané, C. Deranlot, M. Jamet, J.-M. George, L. Vila, and H. Jaffrès, Phys. Rev. Lett. **112**, 106602 (2014).
[31] Y. Liu, Z. Yuan, R. J. H. Wesselink, A. A. Starikov, and P. J. Kelly, Phys. Rev. Lett. **113**, 207202 (2014).

[32] G. Tatara and P. Entel, Phys. Rev. B **78**, 064429 (2008).
[33] H. Kohno, G. Tatara, and J. Shibata, J. Phys. Soc. Jpn. **75**, 113706 (2006).
[34] G. Tatara and H. Fukuyama, J. Phys. Soc. Jpn. **63**, 2538 (1994).
[35] G. Tatara and H. Fukuyama, Phys. Rev. Lett. **72**, 772 (1994).
[36] N. Umetsu, D. Miura, and A. Sakuma, J. Phys. Soc. Jpn. **81**, 114716 (2012).
[37] H. Y. Yuan, Z. Yuan, K. Xia, and X. R. Wang, Phys. Rev. B **94**, 064415 (2016).
[38] J. Foros, A. Brataas, Y. Tserkovnyak, and G. E. W. Bauer, Phys. Rev. B **78**, 140402 (2008).
[39] Z. Yuan, K. M. D. Hals, Y. Liu, A. A. Starikov, A. Brataas, and P. J. Kelly, Phys. Rev. Lett. **113**, 266603 (2014).
[40] G. Tatara, Phys. Rev. B **92**, 064405 (2015).
[41] C. Kittel, *Quantum Theory of Solids* (Wiley, New York, 1963).
[42] K. Nakata and G. Tatara, J. Phys. Soc. Jpn. **80**, 054602 (2011).
[43] Y. Kajiwara, K. Harii, S. Takahashi, J. Ohe, K. Uchida, M. Mizuguchi, H. Umezawa, H. Kawai, K. Ando, K. Takanashi, S. Maekawa, and E. Saitoh, Nature (London) **464**, 262 (2010).
[44] F. D. Czeschka, L. Dreher, M. S. Brandt, M. Weiler, M. Althammer, I.-M. Imort, G. Reiss, A. Thomas, W. Schoch, W. Limmer, H. Huebl, R. Gross, and S. T. B. Goennenwein, Phys. Rev. Lett. **107**, 046601 (2011).
[45] B. Heinrich, C. Burrowes, E. Montoya, B. Kardasz, E. Girt, Y.-Y. Song, Y. Sun, and M. Wu, Phys. Rev. Lett. **107**, 066604 (2011).
[46] C. Burrowes, B. Heinrich, B. Kardasz, E. A. Montoya, E. Girt, Y. Sun, Y.-Y. Song, and M. Wu, Appl. Phys. Lett. **100**, 092403 (2012).
[47] Z. Qiu, K. Ando, K. Uchida, Y. Kajiwara, R. Takahashi, H. Nakayama, T. An, Y. Fujikawa, and E. Saitoh, Appl. Phys. Lett. **103**, 092404 (2013).
[48] X. Jia, K. Liu, K. Xia, and G. E. W. Bauer, Europhys. Lett. **96**, 17005 (2011).
[49] H. L. Wang, C. H. Du, Y. Pu, R. Adur, P. C. Hammel, and F. Y. Yang, Phys. Rev. Lett. **112**, 197201 (2014).
[50] C. Du, H. Wang, F. Yang, and P. C. Hammel, Phys. Rev. Appl. **1**, 044004 (2014).
[51] C. Du, H. Wang, F. Yang, and P. C. Hammel, Phys. Rev. B **90**, 140407 (2014).
[52] H. Wang, C. Du, P. C. Hammel, and F. Yang, Appl. Phys. Lett. **110**, 062402 (2017).
[53] Y. M. Lu, Y. Choi, C. M. Ortega, X. M. Cheng, J. W. Cai, S. Y. Huang, L. Sun, and C. L. Chien, Phys. Rev. Lett. **110**, 147207 (2013).
[54] K. Xia, W. Zhang, M. Lu, and H. Zhai, Phys. Rev. B **55**, 12561 (1997).
[55] M. Caminale, A. Ghosh, S. Auffret, U. Ebels, K. Ollefs, F. Wilhelm, A. Rogalev, and W. E. Bailey, Phys. Rev. B **94**, 014414 (2016).
[56] A. Auerbach, *Intracting Electrons and Quantum Magnetism* (Springer Verlag, 1994).